

REMARKS

Reexamination and reconsideration is respectfully requested in light of the foregoing amendments to the specification and claims and to the following remarks.

Because of numerous amendments to the entire specification, a substitute specification and mark-up copy of the substitute specification are being submitted with this response. No new matter has been added to the specification as amended. Most of the changes involve changing "SEQ ID No." or SEQ ID NO." to --SEQ ID NO:--. Other changes were directed to correcting misspelled words and grammatical errors and for expressing terms with consistent and common nomenclature, e.g., changing "cis-3-hexenol" to --(3Z)-hexenol--; "trans-2-hexanal" to --(2E)-hexanal-- and C6 aldehyde to C₆-aldehyde. As for the change of "linoleic acid" to --linolenic acid-- on page 11 of the specification, support for this change can be found in Fig. 1, page 11, lines 18-19, and Example 4. The addition of "(2E)-hexanal and" is a green note compound and the amendment is supported at page 1, lines 18-20 and page 11, lines 3-11 of the specification and in Fig. 1. Also, the addition of "(3Z)-hexenal and (2E 2E)-hexenal" in the third paragraph on page 5 of the specification is supported by Example 2. It is respectfully requested that the substitute specification be approved and entered.

Claims 1-13 are pending in this application. No claims have been canceled. Claims 4 and 8-13 stand withdrawn from consideration due to a restriction requirement. Applicant notes that the Examiner has made the restriction final. No new claims have been added. However, claims 1-3, 5 and 6 have been amended to correct the notation for "SEQ ID NO:." Also, as set forth below, claims 1, 5 and 6 have been amended to delete the objected to term "about."

Application No.: 10/718,265

Applicant notes the Examiner's consideration of the information cited in the Information Disclosure Statements filed June 21, 2004 and November 21, 2003 as acknowledged in the Office Action Summary.

Rejections for Indefiniteness

Claim 2 stands rejected under 35 U.S.C. § 112, second paragraph, as being indefinite in that the expression “nucleic acid encodes a polypeptide” could be interpreted as including fragments, which the Examiner does not consider the Applicant intended to claim. Under 35 U.S.C. § 112, second paragraph, Applicant is entitled to claim what he regards as his invention. The Examiner has not provided any facts to support her conclusion that Applicant did not intend to include fragments within the scope of his claim. At page 6, lines 10-17, indicates that the proteins with HL activity include fragments. For all of the foregoing reasons, it is respectfully requested that the rejection be reconsidered and withdrawn.

Claims 1-3 and 5-7 stand rejected under 35 U.S.C. § 112, second paragraph, in that the term “about” renders the claims indefinite. The term has been deleted from independent claims 1, 5 and 6. In view of these amendments, the rejection is believed to be overcome. It is respectfully requested that the rejection be reconsidered and withdrawn.

Rejection for Lack of Enablement

Claims 1 and 5-7 stand rejected under 35 U.S.C. § 112, first paragraph, because the specification is not enabling for “any polynucleotide encoding a hydroperoxide lyase having 90% identify to an enzyme of SEQ ID NO: 1.” Applicant respectfully disagrees.

One of the objects of the invention is to use a nucleic acid to encode a polypeptide having at least 90% sequence similarity to SEQ ID NO: 1 (page 3, lines 1-5 of the specification).

Application No.: 10/718,265

In the detailed description of the invention, Applicant sets forth methods for expression, isolation and purification of HL proteins from watermelon and proteins of other plants having at least 90% sequence similarity to SEQ ID NO: 1 (page 6, line 10 to page 8, line 22 of the specification).

The Examiner holds that “the disclosure is limited to the nucleotide and encoded amino acid sequence of only one hydroperoxide lyase.” Applicant disagrees. Fig. 2 is the amino acid sequence of watermelon hydroperoxide lyase (SEQ ID NO: 1). The specification discloses that hydroperoxide lyases have been identified and cloned from several plant species including guava, tomato, *Nicotiana attenuate*, potato, alfalfa, green pepper, *Arabidopsis* and barley which have less than 90% sequence identity to the hydroperoxide lyase in Fig. 2 (page 4, lines 8-23).

The Examiner asserts that “[w]hile recombinant and mutagenesis techniques are known, it is not routine in the art to screen for multiple substitutions or multiple modifications, as encompassed by the instant claims, and the positions within a protein's sequence where amino acid modifications can be made with a reasonable expectation of success in obtaining the desired activity/utility are limited in any protein and the result of such modifications is unpredictable.” The Examiner has not provided any evidence to support this statement or the statement that “one skilled in the art would expect any tolerance to modification for a given protein to diminish with each further and additional modification, e.g. multiple substitutions.” Such conclusions must be supported by evidence. *In re Thrift*, 298 F.3d 1357, 63 USPQ2d 2002, (Fed. Cir. 2002).

With advancement of error-prone polymerase-chained reaction mutagenesis (Joo, H. et al., "Laboratory evolution of peroxide-mediated cytochrome P450 hydroxylation." *Nature* 399(6737): 670-673 (1999)) as well as the DNA shuffling technique (Coco, W.M. et al., , "DNA shuffling method for generating highly recombined genes and evolved enzymes," *Nat. Biotech*

19(4): 354-359 (2001)), screening for multiple amino acid modifications is becoming a routine method for obtaining active enzymes with modified sequences and known to the art (copies of the cited references are attached). Since the tolerance to modification for a given protein is so large as evidenced by the disclosure at page 4, lines 8-23 of the specification, a person having ordinary skill in the art could expect to obtain a polypeptide sequence with less than 90% identity to SEQ ID NO: 1 and having hydroperoxide lyase activity mutated from the mentioned polypeptide.

The Examiner holds that the “specification does not support the broad scope of the claims which encompass all nucleic acids encoding any hydroperoxide lyase with 90% identity to the enzymes of SEQ ID NOS: 1 because the specification does not establish: (A) regions of the protein structure which may be modified without effecting hydroperoxide lyase activity; (B) the general tolerance of hydroperoxide lyase to modification and extent of such tolerance; (C) a rational and predictable scheme for modifying any hydroperoxide lyase residues with an expectation of obtaining the desired biological function; and (D) the specification provides insufficient guidance as to which of the essentially infinite possible choices is likely to be successful.” Again, the Examiner has not provided any reasoning from the teachings of the prior art as to why factors (A) to (C) would cause undue experimentation. As for (D), the specification at pages 6 to 8 provides sufficient guidance to prepare and use the hydroperoxide lyase protein without undue experimentation. Further, the Examiner has not provided any cogent scientific reasoning as to why the specification would provide an “essentially infinite possible choices likely to be successful.” Reliance on common knowledge does not fulfill the Examiner's obligation to

Application No.: 10/718,265

cite references in support of his or her conclusion. *In re Lee*, 277 F.3d 1338, 61 USPQ2d 1430 (Fed. Cir. 2002).

The Examiner also asserts that “Applicants have not provided sufficient guidance to enable one of ordinary skill in the art to make and use the claimed invention in a manner reasonably correlated with the scope of the claims broadly including nucleic acids encoding hydroperoxide lyase with an enormous number of amino acid modifications of the hydroperoxide lyase of SEQ ID NOS: 1 and 2” and that “[w]ithout sufficient guidance, determination of hydroperoxide lyase genes having the desired biological characteristics is unpredictable ...”. These assertions are conclusionary at best and are not supported by any evidence of record. The specification at pages 6 to 8 provide adequate guidance and provide reference cites as well as identifying conventional procedures known in the art to express, isolate and purify the hydroperoxide lyase protein with the provision that the encoded peptide provide hydroperoxide lyase activity.

Though the Examiner has argued that the claims 1 and 5-7 are too broad as to encompass any nucleic acid encoding hydroperoxide lyase having 90% identity to an enzyme of SEQ ID NO: 1, it is not the case with cytochrome P450 enzymes, in which the hydroperoxide lyases belong. Cytochrome P450 enzymes share a similar globular structure, but low sequence identity and the conserved domains are small and scattered throughout the length of polypeptides (Werck-Reichhart, D. and R. Feyereisen, "Cytochromes P450: a success story." *Genome Biol.* 1(6): 3003.1-3003.9 (2000)) (copy of the cited reference is attached). Therefore, any regions except for several certain amino acids, such as cysteine involved in heme-binding, can be modified without effecting hydroperoxide lyase activity significantly.

Application No.: 10/718,265

For all of the foregoing reasons, it is requested that the Examiner reconsider and withdraw the rejection under 35 U.S.C. § 112, first paragraph.

Conclusion

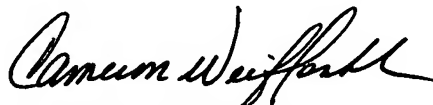
In light of the preceding amendments and remarks, it is believed that claims 1-3, 5 and 7 are patentable over 35 U.S.C. 112, first and second paragraphs. Accordingly, favorable reconsideration of the claims is requested. Allowance of the claims is courteously solicited.

If there are any outstanding issues that might be resolved by an interview or an Examiner's amendment, the Examiner is requested to call Applicants' attorney at the telephone number shown below.

To the extent necessary, a petition for an extension of time under 37 C.F.R. § 1.136 is hereby made. Please charge any shortage in fees due under 37 C.F.R. § 1.17 and due in connection with the filing of this paper, including extension of time fees, to Deposit Account 500417 and please credit any excess fees to such deposit account.

Respectfully submitted,

McDERMOTT WILL & EMERY LLP



Cameron K. Weiffenbach
Registration No. 44,488

600 13th Street, N.W.
Washington, DC 20005-3096
Phone: 202.756.8000 CKW:ckw
Facsimile: 202.756.8087
Date: January 9, 2006

**Please recognize our Customer No. 20277
as our correspondence address.**

photographs (Fig. 2) indicate that excellent sintering had occurred between the iron particles, and that the copper had melted and spread into the iron-particle boundaries forming Fe-Cu solid solutions. The X-ray diffractograms confirm the microscopy observations, and show that the sintered sample contained only a α -iron solid solution single phase.

We also microwave-sintered several powders of pure metals. Only one representative example is described here. Cobalt metal powder was pressed into pellets, and microwave sintered in pure H_2 at 1 atmosphere pressure at various temperatures ranging from 900 to 1,200 °C for 10 minutes. The density reached 8.70 g cm^{-3} at 900 °C to 8.88 g cm^{-3} at 1,000–1,050 °C, and very near theoretical density of 8.89 g cm^{-3} at 1,100–1,200 °C.

These findings have implications for the field of powdered-metal technology. Metal powders are used in industry for a wide range of products and applications. Traditional powder metallurgy involves a process whereby a metal or alloy powder is compacted as a 'green' body and sintered to net shape at elevated temperatures. This process is not labour-intensive, but does consume considerable energy. It conserves materials, and produces high-quality components with reproducible properties. However, the need for materials of high integrity for advanced engineering applications requires newer technologies. The attainment of finer microstructures and near-theoretical densities in special powdered-metal components is still elusive and challenging. Increasing cost is also a concern. The microwave processing method reported here may offer fine microstructures and better properties in powdered-metal products at lower cost. The main reason why the microwave process yields better mechanical properties is two-fold, especially in the case of powdered metals: it produces finer grain size, and the shape of the porosity (if any) is different from that generated during conventional heating. In microwave-processed powdered-metal samples we observed round-edged porosities, producing higher ductility and toughness.

The implications for the fundamental science of microwave-materials interaction are less clear. What is certain from this work and that of Willert-Porada¹⁴ on ceramic sintering is that these interactions are more complex than hitherto suspected. The following factors, at least, contribute significantly to the total microwave heating of powdered metals (object shape and size are also well-known to play a part, but have not been quantified in detail). First, the microwave field generated by a magnetron and the existence of an automatic cut-off mechanism to avoid burn-out due to reflected power. Second, the presence of SiC susceptor rods—taking up only a small fraction of the total space. Third, the existence of a cylindrical insulation package made of aluminosilicate fibres essentially transparent to 2.45-GHz radiation at room temperature, surrounding an alumina tube. Last, the size and nature of the sample placed in the centre of the alumina tube (see Fig. 1).

How the microwave energy absorption is divided between the susceptors, insulation, and sample is a generic issue for all microwave processing, and we consider it in more detail in Supplementary Information. This analysis shows that there is no complete theory to explain even the simplest case of sintering of a ceramic. Furthermore, Cherradi *et al.*²¹ recently claimed that in most ceramics the dielectric loss mechanism was a minor contribution to the power absorbed compared to the induction losses caused by eddy currents. These authors also attribute the heating—they did no sintering—of metals also to eddy-current losses from the electric field. Their evidence, obtained using samples of different size and shape in different orientations, supports the role of such eddy-current losses as a major contributor to the heating of metals. However, all their experiments were done in a single-mode cavity where the orientation of the electric and magnetic fields can be fixed. All our work was done in multimode cavities where the situation is much less determined; but the role of the electric field cannot be ignored.

Another possible significant contribution to the absorption of microwave power, on which much theoretical work has been done²², is multiple scattering in powdered assemblages; this is especially applicable to ceramics and higher microwave frequencies. □

Received 9 October 1998; accepted 20 April 1999.

- Clark, D. & Sutton, W. H. Microwave processing of materials. *Annu. Rev. Mater. Sci.* 26, 299–331 (1996).
- Schiffman, R. F. Commercializing microwave systems: Paths to success or failure. *Ceram. Trans.* 59, 7–17 (1995).
- Katz, J. D. Microwave sintering of ceramics. *Annu. Rev. Mater. Sci.* 22, 153–170 (1992).
- Sutton, W. Microwave processing of ceramics: an overview. *Mater. Res. Soc. Symp. Proc.* 269, 3–19 (1992).
- Sutton, W. Microwave processing of ceramic materials. *Am. Ceram. Soc. Bull.* 68, 376–386 (1989).
- Fang, Y., Agrawal, D. K., Roy, D. M. & Roy, R. Fabrication of transparent hydroxyapatite ceramics by microwave processing. *Mater. Lett.* 23, 147–151 (1995).
- Agrawal, D. K., Fang, Y., Roy, D. M. & Roy, R. *Mater. Res. Soc. Symp. Proc.* 269, 231–236 (1992).
- Fang, Y., Agrawal, D. K., Roy, D. M. & Roy, R. Fabrication of porous hydroxyapatite ceramics by microwave processing. *J. Mater. Res.* 7, 490–494 (1992).
- Fang, Y., Roy, R., Agrawal, D. K. & Roy, D. M. Transparent mullite ceramics from diphasic aerogels by microwave and conventional processing. *Mater. Lett.* 28, 11–15 (1996).
- Fang, Y., Agrawal, D. K., Roy, D. M. & Roy, R. Microwave sintering of calcium strontium zirconium phosphate ceramics. *Ceram. Trans.* 36, 109 (1993).
- Fang, Y., Agrawal, D. K., Roy, D. M. & Roy, R. Microwave sintering of hydroxyapatite-based composites. *Ceram. Trans.* 36, 397 (1993).
- Roy, R., Agrawal, D., Cheng, J. P. & Mathis, M. Microwave processing: triumph of applications-driven science in WC-composites and ferroic titanates. *Ceram. Trans.* 80, 3–26 (1997).
- Cheng, J. P., Agrawal, D. K., Komarneni, S., Mathis, M. & Roy, R. Microwave processing of WC-Co composites and ferroic titanates. *Mater. Res. Innov.* 1, 44–52 (1997).
- Gerdts, T. & Willert-Porada, M. *Mater. Res. Soc. Symp. Proc.* 347, 531–537 (1996).
- Walkiewicz, J. W., Kazonich, G. & McGill, S. L. Microwave heating characteristics of selected minerals and compounds. *Min. Metall. Processing* 5, 39–42 (1988).
- Willert-Porada, M., Gerdts, T., Rodiger, K. & Kolaska, H. Einsatz von Mikrowellen zum Sintern pulvermetallurgischer Produkte. *Metall* 50, 744–752 (1996).
- Nishitani, T. Method for sintering refractories and an apparatus therefor. US Patent No. 4147911 (1979).
- Whittaker, A. G. & Mings, D. M. Microwave-assisted solid-state reactions involving metal powders. *J. Chem. Soc. Dalton Trans.* 2073–2079 (1995).
- German, R. M. *Sintering Theory and Practice* (Wiley, New York, 1996).
- Gedevanishvili, S., Agrawal, D. & Roy, R. Microwave combustion synthesis and sintering of intermetallics and alloys. *Mater. Sci. Lett.* (submitted).
- Cherradi, A., Desgardin, G., Provost, J. & Raveau, B. Electric magnetic field contributions to the microwave sintering of ceramics. In *Electrocera IV* Vol. II, (eds. Wasner, R., Hoffmann, S., Bonnenberg, D. & Hoffmann, C.) 1219–1224 (RWTH, Aachen, 1994).
- Shanker, B. & Lakhtakia, A. Extended Maxwell Garnett formalism for composite adhesives for microwave-assisted adhesion of polymer surfaces. *J. Compos. Mater.* 27, 1203–1213 (1993).

Supplementary information is available on Nature's World Wide Web site (<http://www.nature.com>) or as paper copy from the London editorial office of Nature.

Acknowledgements. We thank J. Kosco for providing powdered-metal components. We also thank the approximately 20 corporations that supported the early stages of this work, which is now supported by the Electric Power Research Institute, the Keystone Powder Metal Company and the Ben Franklin Technology Center.

Correspondence and requests for materials should be addressed to D.A. (e-mail: dx44@psu.edu).

Laboratory evolution of peroxide-mediated cytochrome P450 hydroxylation

Hyun Joo, Zhanglin Lin & Frances H. Arnold

Division of Chemistry and Chemical Engineering 210-41,
California Institute of Technology, Pasadena, California 91125, USA

Enzyme-based chemical transformations typically proceed with high selectivity under mild conditions, and are becoming increasingly important in the pharmaceutical and chemical industries. Cytochrome P450 monooxygenases (P450s) constitute a large family¹ of enzymes of particular interest in this regard. Their biological functions, such as detoxification of xenobiotics and steroidogenesis^{2–5}, are based on the ability to catalyse the insertion of oxygen into a wide variety of compounds⁶. Such a catalytic transformation might find technological applications in areas ranging from gene therapy and environmental remediation to

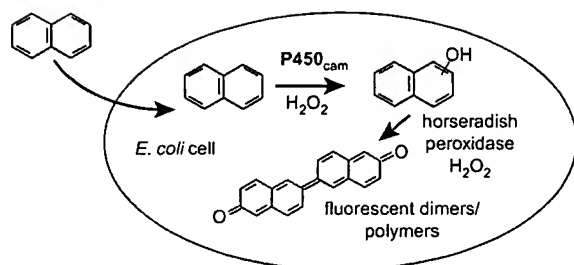


Figure 1 Reaction scheme for detection of active P450_{cam} variants using HRP to generate fluorescent products. The aromatic substrate (here, naphthalene) is taken up by the cells, where it is hydroxylated by the oxygenase. The products of this reaction are oxidatively coupled by HRP, also expressed in the *E. coli*. The product of the coupling reaction is highly fluorescent, and emits at a longer wavelength, relative to the naphthol.

the selective synthesis of pharmaceuticals and chemicals⁷⁻¹⁰. But relatively low turnover rates (particularly towards non-natural substrates), low stability and the need for electron-donating cofactors prohibit the practical use of P450s as isolated enzymes. Here we report the directed evolution¹¹ of the P450 from *Pseudomonas putida* to create mutants that hydroxylate naphthalene in the absence of cofactors through the 'peroxide shunt' pathway^{12,13} with more than 20-fold higher activity than the native enzyme. We are able to screen efficiently for improved mutants by coexpressing them with horseradish peroxidase, which converts the products of the P450 reaction into fluorescent compounds amenable to digital imaging screening. This system should allow us to select and develop mono- and di-oxygenases into practically useful biocatalysts for the hydroxylation of a wide range of aromatic compounds.

Dramatic improvements in cofactor regeneration schemes using a second, coupled enzyme such as formate dehydrogenase have led to the wider use of redox enzymes for chemical synthesis^{14,15}. But coupled enzyme cofactor regeneration is not practical for redox reactions that require multiple proteins (that is, most monooxygenases and dioxygenases). Furthermore, cofactor regeneration requires a second enzyme and a second substrate, and generates a product which must be separated from the desired product. The practical utility of the synthetically versatile P450s would be significantly expanded if we could eliminate the need for a cofactor altogether. Our desire to create practical single-enzyme hydroxylation catalysts led us to attempt to create cytochrome P450s that efficiently utilize hydrogen peroxide (H₂O₂) in lieu of dioxygen and NADH. No longer requiring the P450-associated electron transfer proteins, such catalysts would be extremely simple compared to the natural enzyme systems and could be used in a variety of catalyst forms and reactor configurations.

Horseradish peroxidase (HRP), a highly glycosylated haem peroxidase with four disulphide bridges¹⁶, is not expressed functionally in *Escherichia coli*. However, we generated a variant of HRP that is expressed in active form by directed evolution of the native HRP gene¹⁷. In this variant (HRP1A6), asparagine 255 (a glycosylation site in the native enzyme) is replaced by aspartic acid, a replacement that presumably assists folding in the non-native environment. *E. coli* expressing the monooxygenase cytochrome P450_{cam} from *P. putida*¹⁸ together with HRP1A6 become brightly fluorescent in the presence of naphthalene and H₂O₂ (Figs 1 and 2).

The natural substrate of cytochrome P450_{cam} is camphor; the enzyme shows only weak activity towards naphthalene¹⁹. Approximately 200,000 random mutants of cytochrome P450_{cam} produced by mutagenic polymerase chain reaction (PCR) and coexpressed with HRP1A6 were screened for activity on naphthalene and hydrogen peroxide by fluorescence digital imaging. The fluorescence values of 32,000 clones from this library are plotted in descending order in Fig. 3. Although most of the mutants utilizing

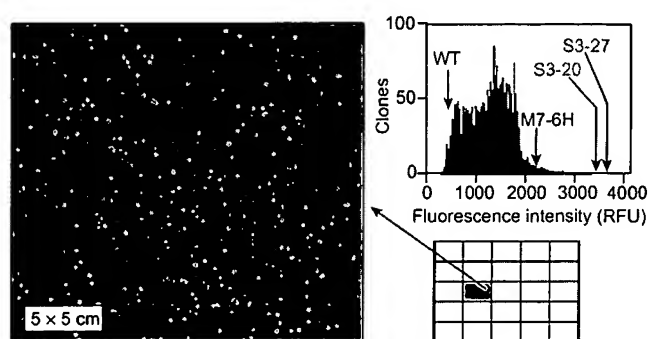


Figure 2 Results of fluorescence measurements. Fluorescence digital (pseudo-colour) image of a portion of a plate with colonies of *E. coli* BL21 (DE3) cells expressing cytochrome P450_{cam} and HRP and containing naphthalene (6 mM) and H₂O₂ (30 mM). Fluorescent products of the HRP coupling reaction are quantified by intensity measurement (see Methods). Histogram on the right side shows the fluorescence values of ~70,000 clones from the library created by StEP recombination of five improved P450_{cam} genes from the first generation (RFU, relative fluorescence units). The fluorescence values of wild-type (WT), improved first-generation variant M7-6H and improved second-generation variants S3-20 and S3-27 are indicated. Large libraries of P450_{cam} variants (here, ~20,000 colonies per plate) can be screened for improved activity, stability or changes in reaction selectivity.

the peroxide shunt pathway are less active than wild type or show no activity at all, a relatively large number show higher levels of fluorescence, indicating higher monooxygenase activity. The fluorescence intensities of control cells either remained constant (host strain with no HRP or P450_{cam}) or showed only a small increase with time (cells expressing the enzymes, but without added naphthalene or H₂O₂, and cells expressing HRP or P450_{cam} singly with naphthalene and H₂O₂; H.J., A. Arisawa, Z.L. and F.H.A., manuscript in preparation).

Three clones with enhanced fluorescence were selected for growth and confirmation of the enhanced activity towards naphthalene in a whole-cell assay. Clone M7-6H showed an 11-fold increase in activity compared to wild-type P450_{cam} (Fig. 3). Two other clones (M7-4H and M7-8H) identified by the digital image scanning also showed at least 5- to 8-fold activity increases. We also assessed the ability of these variants to hydroxylate 3-phenylpropionate (3-PPA) in the whole-cell assay. All three showed improved activities relative to wild-type P450_{cam}; the largest increase was 3.2 fold, for M7-6H. The increased activity of mutant M7-8H was confirmed for the purified enzyme: specific activities of wild-type and M7-8H P450_{cam} were approximately 9 and 70 units (see Methods), respectively, in line with the result from the whole-cell assay.

DNA sequencing revealed the following amino-acid substitutions: E331K (M7-4H); R280L and E331K (M7-6H); E331K and C242F (M7-8H). All three improved P450s have the E331K mutation, which is located in a type I β -turn between the K' helix and a segment often referred to as the 'meander'^{20,21}. Mutation R280L is in the K helix. Cysteine 242 is at the edge of the proximal haem pocket in the I helix; its replacement with phenylalanine may serve to protect the enzyme from rapid inactivation by hydrogen peroxide²². We can offer no simple rationalization for the R280L and E331K mutations. Near, but not in, the distal (peroxide and ligand binding) pocket, they may serve to improve interactions with either the peroxide or the aromatic substrate. Directed evolution is powerful precisely for this ability to identify mutations that influence enzyme activity through subtle, longer-range interactions¹¹.

In the presence of hydrogen peroxide, HRP catalyses the oxidative coupling of a wide variety of phenols and catechols (>140) to generate coloured and fluorescent materials²⁴. This approach is therefore generally useful for screening both mono- and dioxygenases for their ability to hydroxylate an array of aromatic

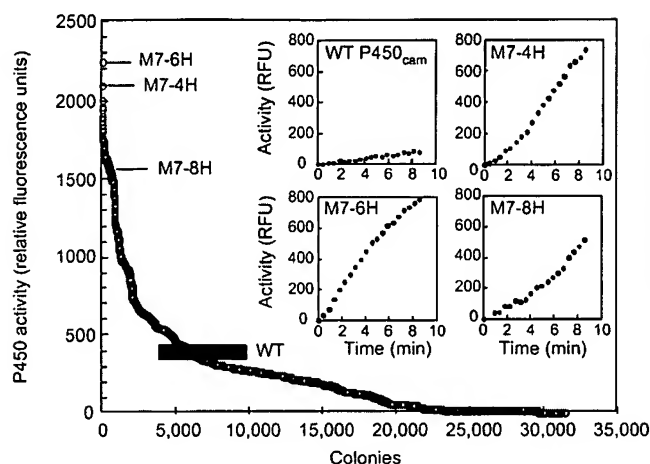


Figure 3 Fluorescence values of *E. coli* clones expressing HRP and random mutants of P450_{cam} in the presence of naphthalene and H₂O₂. Naphthalene hydroxylation activities, as measured by the total fluorescence generated during a fixed incubation period, are plotted in descending order. Total fluorescence of clones expressing wild-type P450_{cam} is also indicated. Insets, activities of selected clones grown in 50-ml cultures, as measured by fluorescence generation (RFU, relative fluorescence units). Wild-type, 9.2 RFU min⁻¹; M7-4H, 84.1; M7-6H, 86.7; M7-8H, 53.1.

compounds. We expect that some subset of the enzymes that are able to utilize the peroxide shunt pathway efficiently to hydroxylate aromatic substrates will also insert oxygen into other substrates, including alkanes and alkenes. These enzymes could be identified by further screening of the reduced libraries (for example, by liquid chromatography/mass spectrometry, LC/MS). Furthermore, the ultraviolet-visible absorption and fluorescence properties of the products of the HRP reaction can be quite distinct for different hydroxylated products, offering the potential to distinguish oxygenases with different regiospecificities. *In vitro* HRP-catalysed polymerization of various naphthol isomers (1- and 2-) and dihydroxylated naphthalenes (DHN) (1,5-, 1,3-, 2,3- and 2,7-DHN) generates a variety of fluorescent products, with dark blue (430–460 nm), blue-green (495 nm), yellow (580 nm) and orange-red (620 nm) fluorescence. A combination of 1- or 2-naphthol and 2,7-DHN produces a red fluorescent product (620 nm), while combining 1,5-DHN with 2,7-DHN or 2-naphthol produces pink or yellow fluorescence, respectively. 1,3-DHN itself shows pink fluorescence; its polymerization with 1-naphthol increases the intensity and shifts the wavelength to the red. The emission spectra of the products depend on the relative molar ratios of the reactants.

Bacteria expressing wild-type P450_{cam} generate only blue fluorescence (460 nm), corresponding to the conversion of naphthalene to 1- or 2-naphthol. Bacteria expressing the P450_{cam} mutants, however, generate a palette of colours (Fig. 4), reflecting the altered regiospecificities of the P450_{cam}-catalysed hydroxylations. Thin layer chromatography and mass spectrometry performed on the products of the whole-cell reaction showed that wild-type P450_{cam} produces primarily 1-naphthol, with a small amount of 1,3-DHN (1-naphthol:1,3-DHN~4.5 : 1). In contrast, 'pink' mutant P-67 produces much more of the dihydroxy-compound (1-naphthol:1,3-DHN~1 : 2). By generating and characterizing P450s with altered substrate and reaction regiospecificities, we should be able to ascertain the molecular determinants of enzyme specificity in this important class of enzymes.

Genes encoding improved P450 variants can be recombined by DNA shuffling methods^{24,25} or further mutated in additional cycles of directed evolution to generate further improved enzymes²⁶. A second-generation P450_{cam} library prepared by staggered extension process (StEP) *in vitro* recombination²⁵ of five improved variants

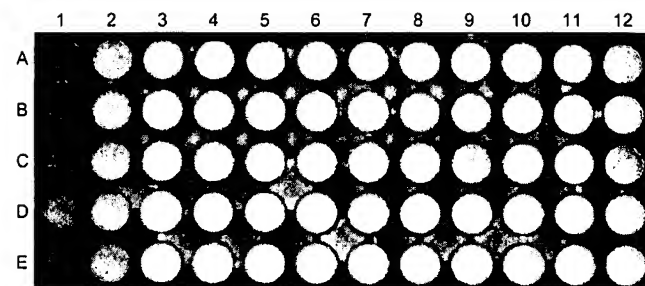


Figure 4 Different colours generated by bacteria expressing HRP and selected P450_{cam} mutants indicating changes in regiospecificity of naphthalene hydroxylation. The first column on the left side (rows A–E) contains control strain *E. coli* BL21 (DE3). The second column contains cells expressing wild-type P450_{cam}. The remaining 50 wells contain different P450_{cam} variants selected by fluorescence image scanning.

has yielded several variants with ~20-fold improvements in naphthalene hydroxylation activity over wild-type. The results of screening this second-generation library are shown in Fig. 2. Two clones isolated from this library are 19- and 21-times more active than wild-type in the whole-cell assay (4 ml culture).

With further evolution of P450s, we would be able to explore the limits of P450-catalysed aromatic hydroxylation via the peroxide shunt pathway. Furthermore, we anticipate that we would be able to identify and evolve thermostable P450s by comparing residual activity after incubation at elevated temperature to initial activity, just as we have done recently to convert a mesophilic esterase²⁷ and protease²⁸ into their thermophilic counterparts. This powerful, simple evolution system should allow us to generate a variety of practical biocatalysts for this useful chemical transformation. It could also be used to screen genetic libraries isolated from the environment for aromatic hydroxylation catalysts.

Cytochrome P450s have presumably evolved by divergent evolution from an ancestral enzyme into a large family of monooxygenases that utilize molecular O₂ as an oxygen source¹. Although the atmosphere of the early Earth contained little or no molecular oxygen, it was relatively rich in H₂O₂ and peroxygenated organic chemicals^{29,30}. The ancient ancestors of today's P450s may have in fact relied on H₂O₂ as the oxygen donor. It is possible that cytochrome P450s that have evolved in the laboratory to function using hydrogen peroxide rather than O₂ could allow us to recreate the functions of these ancestral enzymes. □

Methods

Coexpression of P450_{cam} with HRP. *P. putida* cytochrome P450_{cam} and HRP were coexpressed in *E. coli* BL21(DE3) cells using vectors P450_{cam}-pCWori(+) (provided by P. R. Ortiz de Montellano) and pETpelBHRP1A6Kan. The plasmid backbone of pCWori(+) contains a double *P*_{tac} promoter and an ampicillin resistance coding region. The gene for HRP1A6 was restricted from pETpelBHRP1A6 (ref. 17) and cloned into the kanamycin resistant vector pET26b(+) (Novagen), yielding pETpelBHRP1A6Kan. Intracellular coexpression of P450_{cam} and HRP1A6 was established on agar/terrific broth (TB) plates supplemented with 0.5 mM isopropyl β-D-thiogalactopyranoside, 0.2 mM thiamine, 1 mM δ-aminolevulinic acid and FeCl₃ trace elements. Cultures were seeded onto agar/TB plates supplemented with 100 μg ml⁻¹ ampicillin and 30 μg ml⁻¹ kanamycin, and were grown at 37 °C for 6 h; the incubation temperature was then lowered to 30 °C. After 16 h, the colonies were replicated using a nitrocellulose membrane and transferred onto fresh M9 agar (with 10% (w/v) glucose, 5% (v/v) ethanol) plates containing 6 mM naphthalene and 10 mM (first generation) or 30 mM (second generation) hydrogen peroxide for screening by fluorescence image analysis. Cell viability is >99% for a 6 h reaction in the first generation.

Screening by digital imaging. Fluorescence images were digitally scanned (H.J., A. Arisawa, Z.L. and F.H.A., manuscript in preparation) at 460 nm

wavelength using Eagle Eye II and a top-mounted 350-nm ultraviolet illuminator (Stratagene). Automated colony detection and individual fluorescence intensity measurements were performed using Optimas 5.0 image analysis software (Optimas) with a weighted score of 27,000 grey scale. A blue band-pass filter (430–470 nm), 4× lens zoom level, and 1/10 s CCD exposure time were used. Typical colony diameters were ~0.4–0.8 mm. Scanned images were further processed by configuring overall thresholding, geometry recognition, intensity quantification, global and local segmentation, and cutting edges to reduce background fluorescence.

Hydroxylation activity measurements. Naphthalene and 3-PPA whole-cell hydroxylation activities were measured in 200-μl reactions in a 96-well microtitre plate. P450_{cam} + HRP cells grown in 50-ml flasks were collected by centrifugation (Beckman CS SR) at 3,350 r.p.m. and resuspended in 1 ml of 0.1 M sodium phosphate buffer (pH 9.0). A 50-μl aliquot of the cell solution was added to the reaction mixtures (total 200 μl) containing 25% ethanol, 3-PPA (0.5 mM) or naphthalene (6 mM), and H₂O₂ (10 mM) in the same buffer. Fluorescence was measured in a 96-well microfluorimeter (HTS 7000, Perkin Elmer).

For regioselectivity comparisons, reactions were carried out using cells expressing P450_{cam} and no HRP. Cells grown in 50-ml flasks were collected by centrifugation and gently resuspended in 5 ml of 0.1 M phosphate buffer (pH 9.0) containing 5% (v/v) ethanol, 50 mM naphthalene and 50 mM H₂O₂. After 1 h incubation, the products were extracted with 2 ml of chloroform, and the phases were separated by centrifugation. Residual proteins and salt were removed by ethanol precipitation (3×). The final extracts were spotted on a thin-layer silica plate (Kieselgel 60F₂₅₄, Merck, Darmstadt, Germany) and developed with 94% (v/v) chloroform/methanol. Spots corresponding to 1-naphthol and 1,3-DHN were identified by comparison to the pure compounds and confirmed using an electrospray ionization-quadrupole ion trap mass spectrometer (LCQ, Finnigan, Bremen, Germany). No other hydroxylated naphthalenes were observed at significant concentrations in the product mixtures. Relative concentrations were determined from the integrated spot densities on the thin layer chromatogram (AlphaImager 2000).

Mutagenic PCR and StEP recombination. Mutagenic PCR was performed in a 100 μl reaction as described³¹, using 0.7 mM MnCl₂, 14 pmol of each primer, 5 units of Taq polymerase (Boehringer Mannheim), 0.01% gelatin, 20 pmol of template DNA (P450_{cam}-pCWori(+)). PCR was performed in a thermocycler (PTC200, MJ Research, Waltham, Massachusetts) for 30 cycles (94°C, 30 s; 45°C, 30 s; 72°C, 2 min). Sequences of forward and reverse primers are 5'-CATCGATGCTTAGG AGGTCATATG-3' and 5'-TCATGTTTGACAGCTTATCATCGAT-3'. The StEP method^{25,31} was used to recombine five mutant P450_{cam} genes from the first generation, under slightly mutagenic conditions (0.3 mM MnCl₂).

P450_{cam} purification and assay. Wild-type and M7-8H P450_{cam} were purified as described³². P450 content was estimated by measuring absorbance at 392 nm, with $\epsilon = 104 \text{ mM}^{-1} \text{ cm}^{-1}$. P450 fractions eluted from a Q-Sepharose (Pharmacia) column were pooled (average purity, $A_{392}/A_{280}: 1.4\text{--}1.6$) and washed three times with fresh 10 μM Tris buffer (pH 7.3). Assay conditions were: (200 μl total) 100 μM dibasic phosphate buffer (pH 9.0), 15% (v/v) pure ethanol, 30 μM naphthalene, 1.75 μM HRP (E.C.1.1.1.7, type II; Sigma), 100 μM H₂O₂, 0.031 μM (or 0.282 μg) purified P450. Fluorescence at 465 nm (excitation at 350 nm) was measured in a 96-well microfluorimeter. One unit is defined as the value of 1 a.u. fluorescence increase at 465 nm per min per μg P450.

Received 14 December 1998; accepted 11 May 1999.

- Nelson, D. R. et al. P450 superfamily: update on new sequences, gene mapping, accession numbers and nomenclature. *Pharmacogenetics* 6, 1–42 (1996).
- Cerniglia, C. E. Biodegradation of polycyclic aromatic hydrocarbons. *Biodegradation* 3, 351–368 (1992).
- Cook, D. L. & Atkins, W. M. Enhanced detoxication due to distributive catalysis and toxic thresholds: a kinetic analysis. *Biochemistry* 36, 10801–10806 (1997).
- Waxman, D. J. & Chang, T. K. H. in *Cytochrome P450: Structure, Mechanism and Biochemistry* 2nd edn (ed. Ortiz de Montellano, P. R.) 391–417 (Plenum, New York, 1995).
- Gonzalez, F. J. & Nebert, D. W. Evolution of the P450-gene superfamily—animal plant warfare, molecular drive and human genetic differences in drug oxidation. *Trends Genet.* 6, 182–186 (1990).
- Sono, M., Roach, M. P., Coulter, E. D. & Dawson, J. H. Heme-containing oxygenases. *Chem. Rev.* 96, 2841–2887 (1996).
- Jounaidi, Y., Hecht, J. E. D. & Waxman, D. J. Retroviral transfer of human cytochrome P450 genes for oxazaphosphorine-based cancer gene therapy. *Cancer Res.* 58, 4391–4401 (1998).
- Wackett, L. P., Sadowsky, M. J., Newman, L. M., Hur, H.-G. & Li, S. Metabolism of polyhalogenated compounds by a genetically engineered bacterium. *Nature* 368, 627–629 (1994).
- Faber, K. *Biotransformations in Organic Chemistry* 208–220 (Springer, Berlin, 1997).

- Duport, C., Spagnoli, R., Degryse, E. & Pompon, D. Self-sufficient biosynthesis of pregnenolone and progesterone in engineered yeast. *Nature Biotechnol.* 16, 186–189 (1998).
- Arnold, F. H. Design by directed evolution. *Acc. Chem. Res.* 31, 125–131 (1998).
- Nordblom, G. D., White, R. E. & Coon, M. J. Studies on hydroperoxide-dependent substrate hydroxylation by purified liver microsomal cytochrome P450. *Arch. Biochem. Biophys.* 175, 524–533 (1976).
- Hryciay, E. G., Gustafsson, J.-A., Ingelman-Sundberg, M. & Ernster, L. Sodium periodate, sodium chlorite, organic hydroperoxides and hydrogen peroxide as hydroxylating agents in steroid hydroxylation reactions catalyzed by partially purified cytochrome P450. *Biochem. Biophys. Res. Commun.* 66, 209–216 (1975).
- Hummel, W. & Kula, M.-R. Dehydrogenases for the synthesis of chiral compounds. *Eur. J. Biochem.* 184, 1–13 (1989).
- Seelbach, K. et al. A novel, efficient regenerating method of NADPH using a new formate dehydrogenase. *Tetrahedron Lett.* 37, 1377–1380 (1997).
- Henriksen, A. et al. Structural interactions between horseradish peroxidase C and the substrate benzhydroxamic acid determined by X-ray crystallography. *Biochemistry* 37, 8054–8060 (1998).
- Lin, Z., Thorsen, T. & Arnold, F. H. Functional expression of horseradish peroxidase in *Escherichia coli* by directed evolution. *Biotechnol. Prog.* 15, 467–471 (1999).
- Gunsalus, I. C., Meeks, J. R., Lipscomb, J. D., Debrunner, P. G. & Munck, E. in *Molecular Mechanisms of Oxygen Activation* (ed. Hayaishi, O.) 559–613 (Academic, New York, 1974).
- England, P. A., Harford-Cross, C. F., Stevenson, J.-A., Rouch, D. A. & Wong, L.-L. The oxidation of naphthalene and pyrene by cytochrome P450_{cam}. *FEBS Lett.* 424, 271–274 (1998).
- Poulos, T. L. & Raag, R. Cytochrome P450_{cam}: crystallography, oxygen activation, and electron transfer. *FASEB J.* 6, 674–679 (1992).
- Graham-Lorence, S. & Peterson, J. A. P450s: Structural similarities and functional differences. *FASEB J.* 10, 206–214 (1996).
- Denu, J. M. & Tanner, K. G. Specific and reversible inactivation of protein tyrosine phosphatases by hydrogen peroxide: evidence for a sulfenic acid intermediate and implications for redox regulation. *Biochemistry* 37, 5633–5642 (1998).
- van Deuren, M. P. J., van Rantwijk, F. & Sheldon, R. A. Selective oxidations catalyzed by peroxidases. *Tetrahedron* 53, 13183–13220 (1997).
- Cramer, A., Raillard, S.-A., Bermudez, E. & Stemmer, W. P. C. DNA shuffling of a family of genes from diverse species accelerates directed evolution. *Nature* 391, 288–291 (1998).
- Zhao, H., Giver, L., Shao, Z., Affholter, J. A. & Arnold, F. H. Molecular evolution by staggered extension process (StEP) in vitro recombination. *Nature Biotechnol.* 16, 258–261 (1998).
- Moore, J. C. & Arnold, F. H. Directed evolution of a para-nitrobenzyl esterase for aqueous-organic solvents. *Nature Biotechnol.* 14, 458–467 (1996).
- Giver, L., Gershenson, A., Freskgard, P. O. & Arnold, F. H. Directed evolution of a thermostable esterase. *Proc. Natl. Acad. Sci. USA* 95, 12809–12813 (1998).
- Zhao, H. & Arnold, F. H. Directed evolution converts subtilisin E into a functional equivalent of thermolysin. *Protein Eng.* 12, 47–53 (1999).
- McKay, C. P. & Hartman, H. Hydrogen peroxide and the evolution of oxygenic photosynthesis. *Origins Life Evol. Biosphere* 21, 157–163 (1991).
- Samuilov, V. D. Photosynthetic oxygen: the role of H₂O₂. A review. *Biochemistry (Moscow)* 62, 451–454 (1997).
- Zhao, H., Moore, J. C., Volkov, A. A. & Arnold, F. H. in *Manual of Industrial Microbiology and Biotechnology* 2nd edn (eds Demain, A. L. & Davies, J. E.) 597–604 (ASM Press, Washington DC, 1999).
- Unger, B. P., Gunsalus, I. C. & Sligar, S. G. Nucleotide-sequence of the *Pseudomonas-putida* cytochrome P-450_{cam} gene and its expression in *Escherichia coli*. *J. Biol. Chem.* 261, 1158–1163 (1986).

Acknowledgements. We thank J. H. Richards for encouragement and support, P. R. Ortiz de Montellano for discussions, and G. Bandara for assistance with purification. This work was supported by the Biotechnology Research and Development Corporation and by the Office of Naval Research. H.J. received partial support from the Korea Research Foundation.

Correspondence and requests for materials should be addressed to F.H.A. (e-mail: frances@chem.caltech.edu).

Reassessment of ice-age cooling of the tropical ocean and atmosphere

S. W. Hostettler* & A. C. Mix†

* US Geological Survey, 200 SW 35th Street, Corvallis, Oregon 97331-5503, USA

† College of Oceanic & Atmospheric Science, Ocean Administration Building 104, Oregon State University, Corvallis, Oregon 97331-5503, USA

The CLIMAP¹ project's reconstruction of past sea surface temperature inferred limited ice-age cooling in the tropical oceans. This conclusion has been controversial, however, because of the greater cooling indicated by other terrestrial and ocean proxy data^{2–6}. A new faunal sea surface temperature reconstruction, calibrated using the variation of foraminiferal species through time, better represents ice-age faunal assemblages and so reveals greater cooling than CLIMAP in the equatorial current systems of the eastern Pacific and tropical Atlantic oceans⁷. Here we explore the climatic implications of this revised sea surface temperature field for the Last Glacial Maximum using an atmospheric general circulation model. Relative to model results obtained using



DNA shuffling method for generating highly recombined genes and evolved enzymes

Wayne M. Coco^{1*}, William E. Levinson¹, Michael J. Crist¹, Harm J. Hektor¹, Aldis Darzins¹, Philip T. Pienkos¹, Charles H. Squires^{1,2}, and Daniel J. Monticello¹

We introduce a method of *in vitro* recombination or "DNA shuffling" to generate libraries of evolved enzymes. The approach relies on the ordering, trimming, and joining of randomly cleaved parental DNA fragments annealed to a transient polynucleotide scaffold. We generated chimeric libraries averaging 14.0 crossovers per gene, a several-fold higher level of recombination than observed for other methods. We also observed an unprecedented four crossovers per gene in regions of 10 or fewer bases of sequence identity. These properties allow generation of chimeras unavailable by other methods. We detected no unshuffled parental clones or duplicated "sibling" chimeras, and relatively few inactive clones. We demonstrated the method by molecular breeding of a monooxygenase for increased rate and extent of biodesulfurization on complex substrates, as well as for 20-fold faster conversion of a nonnatural substrate. This method represents a conceptually distinct and improved alternative to sexual PCR for gene family shuffling.

The fundamental goal of gene family shuffling is the generation of diverse gene libraries in which parental sequence polymorphisms are randomly recombined. Current DNA shuffling methods generate chimeric libraries with an average of four or fewer crossovers per gene. Increasing the crossover frequency in shuffled libraries would rapidly expand the diversity of allelic permutations created, generating otherwise inaccessible variants. Another way of exploring alternative combinations of sequence polymorphisms is to effect more frequent "fine-resolution" recombination between closely spaced parental alleles. Progress toward both of these goals has proved difficult using the "sexual PCR" gene shuffling method¹⁻⁶ as well as the "staggered-extension process"^{7,8}.

We report here the development of an *in vitro* recombination method termed "random chimeragenesis on transient templates" (RACHITT). This method employs no thermocycling, strand switching, or staggered extension, but rather the trimming, gap filling, and ligation of parental gene fragments hybridized on a transient DNA template (Fig. 1). For these studies we used *dszC* genes encoding dibenzothiophene monooxygenase (DBT-MO), which catalyzes the first and limiting step of the *dszABCD* diesel biodesulfurization pathway. This pathway is being improved for use in refinery-level biodesulfurization of fossil fuels, as well as for production of chiral sulfoxides and alkylaryl sulfonate surfactant intermediates. We selected evolved enzymes that combined and improved on the parents' rates of substrate oxidation, as well as on their substrate range/affinity for a complex mixture of hydrophobic substrates. Previous extensive efforts at random mutagenesis of the target genes had yielded no detectable improvements in our assays. We thus sought to develop a method that would generate rapid improvements in protein function where random mutagenesis could not. In addition to meeting this goal, our results indicate that the RACHITT method has established new benchmarks in both the frequency and resolution of recombinatory crossovers in gene-family-shuffled libraries.

Results

Construction and characterization of the chimeric *dszC* library. The *dszC* genes from *Rhodococcus erythropolis* IGTS8 (ref. 9) and

Nocardia asteroides A3H1 (ref. 10) are 1.25 kilobases in length and 89.9% identical (differing by 127 nucleotides, including a single codon deletion). They encode proteins differing at 38 residues. DBT-MO from A3H1 has higher substrate affinity and/or substrate range for otherwise poorly converted, complex alkylated derivatives of dibenzothiophene (C_x-DBTs)^{10,11}. The DBT-MO from IGTS8 has a higher specific reaction rate for sparsely alkylated DBTs. The RACHITT method, outlined in Figure 1, was used to recombine the two *dszC* homologs. The resulting chimeric library was cloned and introduced into a nondesulfurizing *Rhodococcus* host. The presence of active chimeras in the library was verified by selection on agar plates containing diesel or the model desulfurization substrate, DBT, as the sole sulfur source.

Restriction fragment length polymorphism (RFLP) analysis of 38 selected and unselected isolates at four sites revealed the presence of 88% of the possible fragmentation patterns. This result, and the number of representatives observed for each class (ranging from 0 to 7), approached random reassortment and complete allelic dislinkage. In 27,588 bases of DNA sequenced from unselected library clones, only highly recombinant genes were found (Fig. 2). These clones contained an average of 14.0 recombinational crossovers per gene. Additionally, no unshuffled parental clones or duplicate occurrences ("siblings") were found (i.e., 100% recombinant yield). Remarkably, in the 22 randomly chosen genes sequenced, 89 of the 309 observed recombinatory crosses can be traced to regions of sequence identity of 10 or fewer bases, and more than half this number to patches of 5 or fewer bases (Fig. 3).

In the 27,588 bases sequenced, 25 spontaneous mutations were found. This rate of 1 mutation per 1,103 bases is well within the number of spontaneous mutations expected from the one and two rounds of PCR used to generate fragment DNA and template DNA, respectively, and the final round of PCR used to amplify the chimeric products. This conclusion was derived using the Poisson analysis of Kunkel and Eckert¹², which resulted in a calculated Taq polymerase error rate for the above amplifications of one misincorporation per 35,000 bases polymerized. Supporting the PCR-derived origin of

¹Enchira Biotechnology Corporation, 4200 Research Forest Drive, The Woodlands, TX 77381. ²Current address: The Dow Chemical Company, 5501 Oberlin Dr., San Diego, CA 92121. *Corresponding author (wcoco@enchira.com).

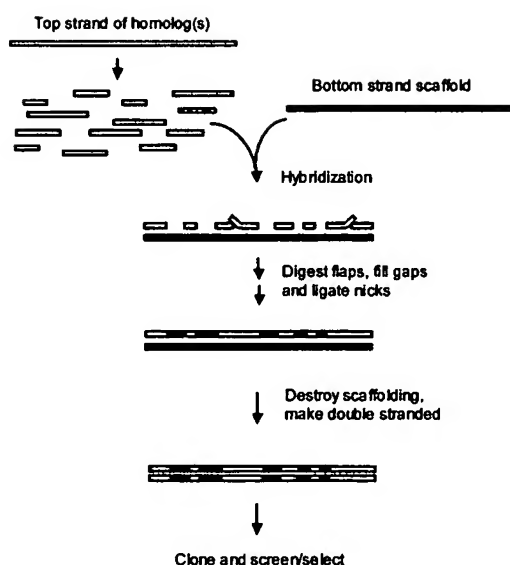


Figure 1. Random chimeragenesis on transient templates (RACHITT). A uracil-containing *Rhodococcus erythropolis* IGTS8 *dszC* gene was made single-stranded to serve as a transient scaffold template (black bar). This molecule mediates the ordering of *Nocardia asteroides* A3H1 top-strand fragments (white bars) and serves as a template for the filling of gaps. Unhybridized 5' and 3' termini or "flaps" are expected on some annealed fragments because of overlap with adjacent fragments, or because of mismatches with respect to the scaffold, and are trimmed using nucleases. Filling gaps between hybridized fragments allows inclusion of template sequences as mosaic insertions into the nascent chimeric strand. After flap trimming, gap filling, and ligation, the heteroduplexed parental bottom-strand template is rendered nonamplifiable by uracil-DNA-glycosylase treatment and is replaced by homoduplex chimeric bottom strand during PCR.

most spontaneous mutations, the number of mutations found in chimeric regions created by gap filling or brought in as DNase I cleaved fragments corresponded to the number of PCR amplification cycles used to generate the template and fragment parents, respectively. Further, no unexpected insertions, deletions, or rearrangements were detected by DNA sequencing or RFLP analysis of >60 clones. Consistent with our genetic analyses, the 175 phenotypes reflected in Figure 4A indicate the presence of a relatively small fraction of inactive clones in the library. Taken together, these data suggest that the RACHITT procedure itself introduced few additional mutations or gross gene rearrangements.

Screening for improved reaction rate. We isolated proteins with higher rates of substrate turnover by screening library clones in a whole-cell, two-phase microplate format assay. Of 175 unselected clones tested, the six best were confirmed to have significantly higher activity than the parents (Fig. 4A). All six were chimeric by RFLP analysis. Two isolates, designated 4-5 and 6-2, were significantly better than either parent under all tested conditions. A third, 2-3, was better at desulfurizing diesel (Fig. 4B), but not the model compound, DBT. All three were subjected to DNA sequencing (Fig. 2).

Simultaneous improvements in rate and extent of reaction. In a separate experiment, sequential selection and screening of the chimeric library were performed on a low-sulfur diesel substrate to identify variants that simultaneously exceeded both the rate and affinity characteristics of the parents. Diesel oil was deeply biodesulfurized by a *Rhodococcus* strain containing only genes from IGTS8, and then diluted in dodecane until a strain containing only IGTS8 *dsz* genes was no longer able to grow. We then modified this

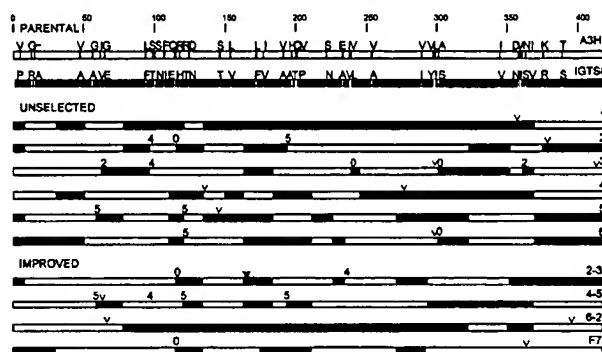


Figure 2. RACHITT generates highly mosaic shuffled proteins. In the top panel are bars representing the entire protein sequence for the two parental DBT-MOs (solid white and solid black). Vertical lines in the parental sequences indicate the position of each of the 38 residues that differ between the parents, including a one-residue deletion (-). Of 22 randomly chosen unselected clones, 6 are shown. The improved clones were selected or screened as described in the text. The F7 clone combined the best rate and affinity phenotype. Spontaneous mutations are indicated by carets (v) above the bars. The locations of recombinational crossovers in regions of 0 to 5 amino acid residue identities are also identified above the bars (0 indicates recombination between adjacent residues). White bars connect A3H1 donated residues that are not interrupted by unique IGTS8 sequences, and will generally correspond to contiguous blocks of sequence donated by one or more A3H1 fragments. The locations of crossovers are parsimoniously depicted at the midpoint of regions of identity between parental differences. The minimum average number of crossovers per protein by this analysis is 9.8 for the unselected clones, but analysis of phenotypically silent differences at the DNA level reveals that 14.0 is the true minimum (see text).

strain by replacing the IGTS8 *dszC* gene with that of A3H1. This modified strain was able to grow and effected measurable additional sulfur oxidation, consistent with the high-affinity phenotype of the A3H1 DBT-MO. We isolated 109 clones after growth selection of the chimeric *dszC* library using the deeply desulfurized, diluted oil. These clones were tested for activity in the microplate format rate assay, and several were found to have acquired the rate of the IGTS8 parent or better (Fig. 5A). The eight most active clones were found to be chimeric by RFLP and/or by DNA sequencing (F7, Fig. 2). This marriage of higher rate and improved extent of substrate oxidation was confirmed and quantified using the more precise shake-flask assays (F7, Figs 4B, 5B). That high rate alone is not enough to provide greater extent of oxidation was shown by the parental phenotypes.

Evolving enzyme substrate specificities. Substrate range analysis of both the parental DBT-MOs and their pathways suggests that organo-sulfur compounds are the natural substrates of the *dsz* pathways^{10,13-16}. To explore whether the chimeric library contained clones evolved for phenotypes unrelated to desulfurization, we attempted to isolate clones with improvements relative to a nitrogen-containing substrate. Because DBT-MO gratuitously catalyzes the slow conversion of indole, yielding the colored product, indigo, we used this as a phenotypic screen for shifts in substrate spectrum. It was expected that a chimeric library from parental enzymes displaying even low-level indole oxidation would include clones with a wide range of indole oxidation activity. This was indeed the case, with library-transformed colonies filling in the phenotype space around and between both parents (Fig. 6). Quantitative assays revealed over 20-fold improvement in indigo production (Fig. 6B). That these were true specificity differences and not mere differences in cellular activity (e.g., expression levels) was supported by the finding that the rate of indigo production from these clones did not correlate with their DBT-MO activity.



RESEARCH ARTICLE

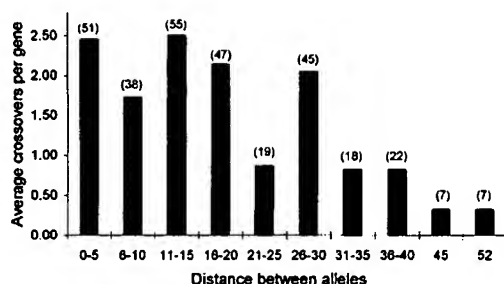


Figure 3. RACHITT-derived chimeric genes exhibit high-frequency recombination at closely spaced parental sequence polymorphisms (alleles). Each of the 309 crossover events is summarized for 22 unselected clones chosen at random for DNA sequencing. Bar height depicts the average number of recombinations per gene in groupings of DNA sequence identity of a given size. The number of recombinations observed in each grouping is shown in parentheses above the bar. Distance between alleles is in nucleotides. Zero distance between alleles indicates recombination between adjacent sequence polymorphisms and occurred a total of three times in unselected clones.

Discussion

The benefits of genetic recombination over random mutagenesis in the rapid evolution of organisms, genes, and proteins are well established¹⁷⁻²¹. "Sexual PCR" and "staggered-extension" PCR are two methods proven to improve proteins by *in vitro* recombination using random chimeragenesis, or "DNA shuffling", and both have been useful in the recombination of mutations in single genes^{4,8}. The recent ITCHY (iterative truncation for the creation of hybrid enzymes) method has been recognized for yielding diverse "head-to-tail" single-crossover chimeras independent of genetic homology, but, as yet, no improved proteins have been reported for this method²². The sexual PCR method of Stemmer, with some variations, has until now been the only *in vitro* method shown to improve proteins by recombination of separately evolved gene homologs in a process called "molecular breeding" or "gene family shuffling"^{1,2,6,23-25}.

A comparison of shuffling methods at the molecular level requires DNA or protein sequence information for all parental

clones, coupled with sequence information for several unselected chimeric progeny. Despite the successes of the method, studies providing these details for gene family shuffling by sexual PCR have reported libraries containing 0–100% background of unshuffled parental wild-type clones and shuffled clones averaging at most four crossovers per round of shuffling (Table 1). DNA sequence and RFLP analyses of RACHITT-generated libraries indicated broad representation among the possible classes of chimeras. Further, no parental genotypes or duplicate occurrences of the same chimeric gene (e.g., siblings) were found by DNA sequencing. We conclude that binding and incorporation of multiple and alternative hybridizing fragments during the chimeragenesis reactions were largely random. Moreover, our results indicated a per-gene average of 14 crossovers, a several-fold higher level of crossovers than reported thus far for other shuffling methods (Table 1). These qualities have more recently allowed us to generate shuffled libraries and evolved clones from 4 to 14 parents simultaneously, including mixed, uncharacterized genes and/or significantly more divergent parental genes (W.M. Coco *et al.*, unpublished data).

In addition, sexual PCR suffers severe linkage effects that make crossovers in regions of identity of <15 bases rare^{4,8} (Table 1). These inefficiencies result in large uninterrupted tracts of sequences from individual parental genes, and a corresponding significant reduction of the combinatorial diversity of parental alleles explored. In the present study, we found, on average, more than four recombinations per gene between alleles spaced 10 or fewer bases apart. In fact, the number of recombinations per gene occurring between even 0–5 bases of uninterrupted sequence identity did not drop off in comparison to the average number of recombinations in any other size category, as shown in Figure 3. This unprecedented high recombinational frequency between closely linked sequence polymorphisms contributes significantly to the generation of random libraries that more fully exploit the allelic diversity inherent in parental proteins.

We attribute the advantages of RACHITT to several features of the method. RACHITT utilizes a single hybridization event, as opposed to the thermocycling steps used in PCR-based methods. The occurrence of misannealed primers and fragments in PCR, and their interference with the generation of a desired amplification

Table 1. Comparison of DNA shuffling methods^a

Shuffling method (modifications)	Target gene(s)	Number of unselected genes analyzed	Average crossovers per chimeric gene ^b	Fine-resolution recombinations per gene ^c	Percentage background (unshuffled parental clones)
RACHITT	Monooxygenase homologs (this work)	22	14.0	2.45	0
Sexual PCR	Dioxygenase homologs ¹	100	0	NR	100
Sexual PCR (single-stranded fragments)	Dioxygenase homologs ¹	50	3.1	NR	86
Sexual PCR	Thymidine kinase homologs ²⁵	20	NR	NR	15%
Sexual PCR (random-priming)	Subtilisin ³	10	4.1	NA	0
Sexual PCR (high fidelity)	Subtilisin ⁶	10	2	NA	10
Sexual PCR (Mn ²⁺ buffer)	Antibody Fv chain homologs ²	5	3.4	NR	0
Sexual PCR (low-temperature annealing)	Interleukin 1β homologs ⁴	9	1.8	0.44 ^d	NR
Staggered extension (STEP)	Subtilisin E ⁸	10	2.1	NA	0
Staggered extension	Ribonuclease homologs ⁷	32	1.2	NR	53
Staggered extension	Growth hormone homologs ⁷	25	1.0	NR	52

^aResults are included for experiments reporting data for at least two of the four categories. NA, Not applicable (experiments involved mutational variants of a single gene that did not contain alleles with 0–5 bp spacing. NR, None reported.

^bOccasional multiple crossovers within uninterrupted regions of identity cannot be scored. The numbers in this column thus represent the number of detectable crossovers.

^cAverage crossovers per chimeric gene of alleles separated by 0 to 5 intervening identical bases after one round of shuffling.

^dAnnealing took place on dry ice/ethanol to increase pairing in regions of divergence. No improved clones were reported.

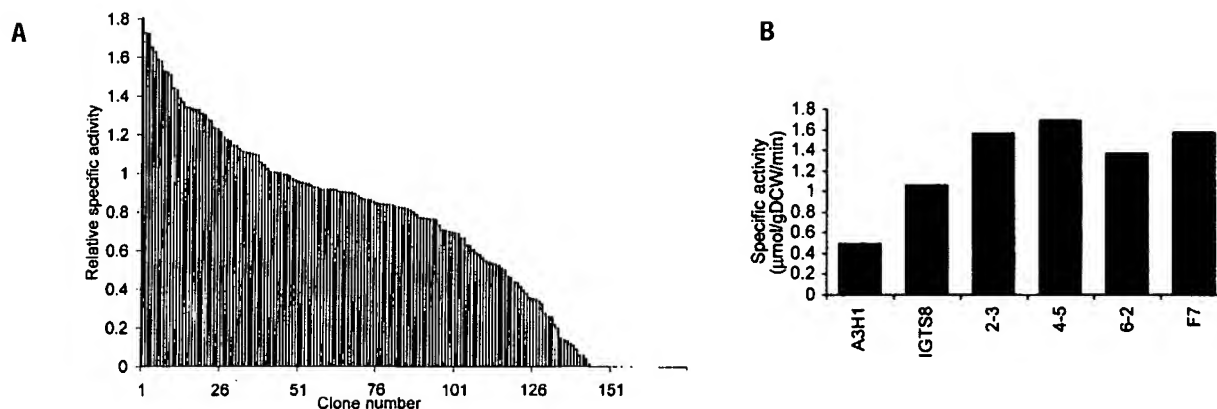


Figure 4. Rate screen of the *dszC* chimeric library reveals improved clones. (A) Unselected clones were screened for rate of sulfite production. Vertical bars represent rate determinations from individual clones. Rates were determined in 96-well microplates and were adjusted for optical density of each culture. The activity of each measured isolate was normalized to the average activity for the rest of the same microplate. The IGTS8 parent possesses an activity of ~1. (Note that this chart depicts unselected clones, not a preselected or active subset.) (B) Shake-flask desulfurization assays with 10% diesel in dodecane (550 p.p.m. sulfur) confirm improved desulfurization. Strains containing parental wild-type A3H1 or IGTS8 DBT-MO were compared to biocatalysts harboring the best evolved *dszC* clones from (A) and from Figure 5B. Flasks were shaken for 60 min at 30°C. The oil phase was then recovered and analyzed for total sulfur content by gas chromatography with sulfur chemiluminescence detection (GC-SCD). Recloning of each open reading frame into the original plasmid vector ruled out contributions from vector-based mutations.

product, is well known. This problem is magnified in the simultaneous amplification of hundreds of randomly cleaved DNA fragments necessary in sexual PCR. As in traditional probe-target solution hybridization reactions, the single hybridization step in RACHITT lends itself to greater binding specificity for DNA fragments of both low and high sequence identity. It also incorporates "flap" trimming to result in duplexed ligatable/extendable ends from otherwise unproductive fragments. Although careful attention to the experimental system can produce selectivity in the ligase chain reaction²⁶, many DNA ligases do allow ligation of mismatched termini²⁶⁻²⁹. Similarly, despite successes with allele-specific PCR, Taq polymerase allows reasonably efficient polymerization from three-fourths of the 12 possible 3'-mismatched termini³⁰. Where flaps were not perfectly trimmed, such low-fidelity reac-

tions appear to have contributed crossovers between adjacent mismatches. In addition, trimming allows incorporation of fragments much smaller than those generated in the DNase I reaction. Ligation of adjacent fragments from the same parent, on the other hand, allows linking of larger stretches from any given parent than were present after DNase I cleavage (Fig. 2). Finally, RACHITT exploits a bottom-strand template from only one parent and only top-strand fragments of other parents. This prevents parental fragments from reannealing to their own complementary strands. In sexual PCR, priming among fragments of the same gene is favored and is known to decrease the number of crossovers and increase the proportion of nonchimeric parents regenerated in recombinant libraries¹. This is especially the case when few homologous genes are available or desired for a given shuffling reaction.

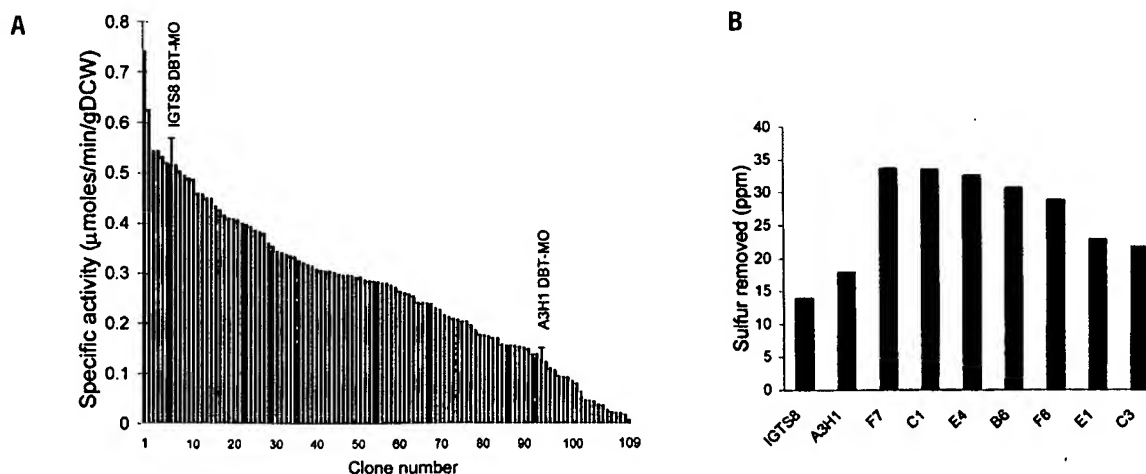


Figure 5. Clones simultaneously improved for both rate and extent of substrate oxidation are identified by sequential selection and screening. (A) Rate screen of the *dszC* chimeric library after preselection for growth on dilute deeply biodesulfurized oil (see text). Rates were adjusted for optical density of each culture and specific activities calculated. (Note that the specific activities calculated in the microplate format were about half of those found in the shake-flask assay (see Fig. 4B, isolate F7).) (B) Desulfurization of diluted, deeply biodesulfurized diesel. The seven highest rate clones from (A) were transferred to flasks containing deeply biotreated and diluted diesel (see text). After incubation for 24 h, the oil was analyzed by GC-SCD.

RESEARCH ARTICLE

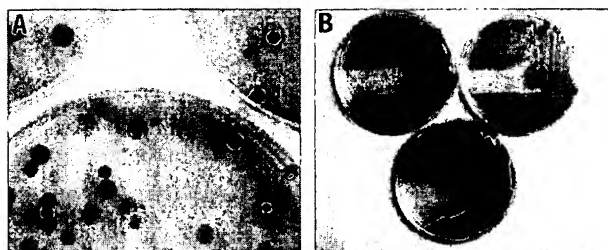


Figure 6. Evolution of substrate range. (A) A high level of phenotypic diversity is generated from the chimeric library. The *Rhodococcus*-borne chimeric *dszC* library was plated to rich medium, grown three days, subjected to indole vapors 3 h, and incubated five additional days. The amount of color development in plates containing *dszC* from strain IGTS8 (top left) or from A3H1 (top right) was reliably uniform, with the former producing little indigo and the latter somewhat more. Note the wide variability among the unselected library transformants (bottom). This "filling in" of phenotype space between and beyond both parents is what is expected from a diverse chimeric library. (B) A strain determined to be over 20-fold improved for indole oxidation in spectrophotometric assays was treated as above, but subjected to indole vapors and grown for only two days (lower plate) along with otherwise isogenic strains containing the parental A3H1 and IGTS8 *dszC* genes (upper left and right plates, respectively).

The diversity of chimeric phenotypes generated by RACHITT was evident in experiments assessing both rate of desulfurization (both with and without dilute oil preselection) and rate of indole oxidation. In the three relevant experiments, a continuous range of activity values was observed, from better than both parents to worse, indicating a complex inheritance pattern (e.g., contributions from many unlinked or partially linked loci and/or from alternate permutations of alleles). Such a wide range of activities is expected and is indeed a hallmark of successfully shuffled libraries²¹. This spectrum of phenotypic diversity and the relatively low frequency of inactive clones allowed identification of isolates with 60–320% improvement in flux through the pathway compared with the two parents after screening relatively few clones (175 unselected clones, or <0.5% of the generated library). Where we did apply a growth selection, twofold improvement in the amount of sulfur oxidized from a deeply biotreated diesel was easily obtained compared with either parent (Fig. 5B). No such improvements were seen after random mutagenesis by several methods, followed by similar screens (data not shown). Despite this preselection of the library for clones expressing the extent phenotype, more than threefold higher rates than the A3H1 "extent" parent were also captured in ~1% of these same proteins (Figs 4B, 5A). This demonstrates that clones simultaneously evolved in both rate and extent of substrate oxidation were created at relatively high frequency in this inter-genus shuffled library. The similar fraction of high-rate clones, regardless of preselection for extent of biodesulfurization, together with the lack of steps or jumps throughout the range of observed activities, indicate that these two phenotypes are complex, independent, and genetically not significantly linked. Under steady-state conditions in whole cells, the oxidation product of the A3H1 or IGTS8 DBT-monooxygenases, DBT-sulfone, remains undetectable (<0.1 μmol) because of the high rates of reaction of the downstream-pathway enzymes. An increase in steady-state DBT-sulfone concentration of at least 16 fold was observed in pathways containing the shuffled *dszC* genes (data not shown). This indicates that the improvements in pathway performance have significantly mitigated the rate limitation of this first step in the *dszABCD* pathway, and that additional significant improvements to this enzyme may not be detectable by the employed two-phase, whole-pathway, whole-cell screen³¹. Indigo formation rates more than 20-fold higher than either parent, however, were readily detected using the same shuffled library.

In summary, the RACHITT method resulted in undetectable levels of siblings, relatively few inactive proteins, and no unshuffled parental clones. It also yielded an unprecedented predominance of more highly mosaic clones and the ability to effect frequent recombination between close and even adjacent alleles. The improvements observed were in the key mechanisms that determine the diversity and evolutionary potential of gene-shuffled libraries. They allow exploration of more diverse permutations of multiple mutations than is possible by other methods. This ability to capture untapped regions of sequence space should facilitate the evolution of proteins having desired characteristics³².

Experimental protocol

RACHITT. Lambda exonuclease-generated *dszC* top strand from A3H1 was partially DNase I digested and isolated (200 fmol, 45–200 nt), and uracil-containing IGTS8 *dszC* bottom-strand scaffold (35 fmol) were prepared by published methods^{23,34}. The quality of these substrates is critical. After hybridization of the above in the presence of 2.5 pmol oligonucleotides that strongly bind the template 5' and 3' termini (65°C, 30 min in Taq ligase buffer), unhybridized 5' termini or "flaps" were cleaved by the flap endonuclease activity of Taq DNA polymerase³⁵ (0.5 units, 65°C, 2 min, in the presence of 20 units Taq DNA ligase). Modifications using hybridization buffers with up to 1 M sodium ion, hybridization times up to 15 h, or hybridization temperatures as low as 40°C were evaluated (data not shown). However, with gene homologs of $\geq 70\%$ DNA sequence identity, no adjustment to the above protocol was necessary. Ligation continued in a reaction in which 3' flaps were digested by the 3'-5' exonuclease activity of Pfu DNA polymerase, which also served to fill gaps (one-twentieth of the above diluted into 10 μl Taq ligase buffer containing 100 μM dNTPs, 1.25 units Pfu polymerase, 0.5 units Taq DNA polymerase, and 10 units Taq DNA ligase, 45°C to 60°C ramp, 30 min). Template was then rendered nonamplifiable by treatment with uracil-DNA-glycosylase (0.5 units, 37°C, 30 min). PCR then amplified double-stranded homoduplex chimeras for cloning. The cloning vector, pEBC1100, was constructed with the *dszABCD* artificial operon and replication origins from *colE1* and pRC1 (ref. 36). The chimeric *dszC* library was cloned to replace the parental *dszC* in pEBC1100 and, after amplification in *Escherichia coli*, transformed into JB55, a nondesulfurizing derivative of strain IGTS8. The number of transformants was 35,000, which set the upper limit for the number of unique clones in this library.

Shake-flask desulfurization assay with deeply biodesulfurized diesel. The seven highest rate clones from Figure 5A were grown in 45 ml of a defined medium with 2% glucose, 50 $\mu\text{g}/\text{ml}$ kanamycin, and 1 mM dimethyl sulfoxide (DMSO). Cell mass was resuspended to $\text{OD}_{600} = 25$, and 9 ml transferred to 50 ml flasks with 3 ml of deeply biotreated and diluted diesel. The cultures were incubated at 30°C at 300 r.p.m. for 24 h. The oil was then analyzed by gas chromatography with sulfur chemiluminescence detection (GC-SCD).

Rate screens. Cultures were grown in mineral medium to $\text{OD}_{600} = 10$ to 20 in 96-well plates, were mixed 1:1 with 20% diesel in dodecane (500 p.p.m. sulfur in the oil), and shaken 30 min at 30°C. The final sulfur-containing pathway product, sulfite, was measured in the aqueous phase using a sulfite oxidase, enzyme-coupled spectrophotometric assay. Hits from the microplate format assay were isolated and cultured in shake flasks to $\text{OD}_{600} = 8$, concentrated to $\text{OD}_{600} = 28$, and placed in Erlenmeyer flasks with 10% diesel in dodecane or 0.6% (wt/vol) DBT in hexadecane (3:1 water:oil ratio). Disappearance of substrates and/or appearance of products were measured as indicated in the figure legends. For indole rate screens, unselected clones were grown in 96-well plates and exposed to 0.25 mM indole overnight. After centrifugation, clones producing the darkest cell pellets were quantified as published³⁷.

Acknowledgments

We thank the Enchira high-throughput screening and analytical chemistry groups for expert technical assistance; G. Mrachko, B. Blattmann, J. Arensdorf, E. Lange, J. Blanton, B. Folsom, U. Coco, J. Bryson, and L. Encell for developing additional assays, assistance with figures, statistical analyses and critical comments on the manuscript.

Received 7 August 2000; accepted 11 January 2001



1. Kikuchi, M., Ohnishi, K. & Harayama, S. An effective family shuffling method using single-stranded DNA. *Gene* **243**, 133–137 (2000).
2. Lorimer, I.A. & Pastan, I. Random recombination of antibody single chain Fv sequences after fragmentation with DNaseI in the presence of Mn²⁺. *Nucleic Acids Res.* **23**, 3067–3068 (1995).
3. Shao, Z., Zhao, H., Giver, L. & Arnold, F.H. Random-priming *in vitro* recombination: an effective tool for directed evolution. *Nucleic Acids Res.* **26**, 681–683 (1998).
4. Stemmer, W.P. DNA shuffling by random fragmentation and reassembly: *in vitro* recombination for molecular evolution. *Proc. Natl. Acad. Sci. USA* **91**, 10747–10751 (1994).
5. Stemmer, W.P. Rapid evolution of a protein *in vitro* by DNA shuffling. *Nature* **370**, 389–391 (1994).
6. Zhao, H. & Arnold, F.H. Optimization of DNA shuffling for high fidelity recombination. *Nucleic Acids Res.* **25**, 1307–1308 (1997).
7. Levichkin, I.V., Shuf'ga, A.A., Kurbanov, F.T. & Kirpichnikov, M.P. A new method of designing hybrid genes—the homolog recombination method. *Mol. Biol. (Mosk)*. **29**, 983–991 (1995).
8. Zhao, H., Giver, L., Shao, Z., Affholter, J.A. & Arnold, F.H. Molecular evolution by staggered extension process (StEP) *in vitro* recombination. *Nat. Biotechnol.* **16**, 258–261 (1998).
9. Piddington, C.S., Kovacevich, B.R. & Rambosek, J. Sequence and molecular characterization of a DNA region encoding the dibenzothiophene desulfurization operon of *Rhodococcus* sp. strain IGTS8. *Appl. Environ. Microbiol.* **61**, 468–475 (1995).
10. Fridrick, C. *et al.* Isolation and characterization of a biodesulfurizing *Nocardia* sp. In *Abstracts of the 99th General Meeting of the American Society for Microbiology*, Abstr. O-23 500. (American Society for Microbiology, Washington, DC; 1999).
11. Levinson, W., Coco, W., Crist, M., Fridrick, C. & Pienkos, P. Directed evolution of DBT monooxygenase using growth on biodesulfurized diesel oil as a selection and screening strategy. In *Abstracts of the Annual Meeting of the Society for Industrial Microbiology*, San Diego, Abstr. P31 128. (Society for Industrial Microbiology, Fairfax, VA; 2000).
12. Eckert, K.A. & Kunkel, T.A. The fidelity of DNA polymerase used in the polymerase chain reactions. In *PCR. A practical approach*. (eds McPherson, M.J., Quirke, P. & Taylor, G.R.) 225–244 (IRL Press, Washington, DC; 1991).
13. Arensdorf, J.J. & Pienkos, P. Biotransformations of model sulfur compounds by *Rhodococcus*. In *Abstracts of the 100th General Meeting of the American Society for Microbiology*, Los Angeles, Abstr. O-24 501. (American Society for Microbiology, Washington, DC; 2000).
14. Lei, B. & Tu, S.C. Gene overexpression, purification, and identification of a desulfurization enzyme from *Rhodococcus* sp. strain IGTS8 as a sulfide/sulfoxide monooxygenase. *J. Bacteriol.* **178**, 5699–5705 (1996).
15. Denome, S.A., Oldfield, C., Nash, L.J. & Young, K.D. Characterization of the desulfurization genes from *Rhodococcus* sp. strain IGTS8. *J. Bacteriol.* **176**, 6707–6716 (1994).
16. Oldfield, C., Pogrebinsky, O., Simmonds, J., Olson, E.S. & Kulpa, C.F. Elucidation of the metabolic pathway for dibenzothiophene desulfurization by *Rhodococcus* sp. strain IGTS8 (ATCC 53968). *Microbiology* **143**, 2961–2973 (1997).
17. Charlesworth, B. Mutation-selection balance and the evolutionary advantage of sex and recombination. *Genet. Res.* **55**, 199–221 (1990).
18. Felsenstein, J. The evolutionary advantage of recombination. *Genetics* **78**, 737–756 (1974).
19. Felsenstein, J. & Yokoyama, S. The evolutionary advantage of recombination. II. Individual selection for recombination. *Genetics* **83**, 845–859 (1976).
20. Kondrashov, A.S. Deleterious mutations as an evolutionary factor: 1. The advantage of recombination. *Genet. Res.* **44**, 199–217 (1984).
21. Minshull, J. & Stemmer, W.P. Protein evolution by molecular breeding. *Curr. Opin. Chem. Biol.* **3**, 284–290 (1999).
22. Ostermeier, M., Nixon, A.E. & Benkovic, S.J. Incremental truncation as a strategy in the engineering of novel biocatalysts. *Bioorg. Med. Chem.* **7**, 2139–2144 (1999).
23. Cramer, A., Raillard, S.A., Bermudez, E. & Stemmer, W.P. DNA shuffling of a family of genes from diverse species accelerates directed evolution. *Nature* **391**, 288–291 (1998).
24. Kumamaru, T., Suenaga, H., Mitsuoka, M., Watanabe, T. & Furukawa, K. Enhanced degradation of polychlorinated biphenyls by directed evolution of biphenyl dioxygenase. *Nat. Biotechnol.* **16**, 663–666 (1998).
25. Christians, F.C., Scapozza, L., Cramer, A., Folkers, G. & Stemmer, W.P. Directed evolution of thymidine kinase for AZT phosphorylation using DNA family shuffling. *Nat. Biotechnol.* **17**, 259–264 (1999).
26. Barany, F. The ligase chain reaction in a PCR world. *PCR Methods Appl.* **1**, 5–16 (1991).
27. Luo, J., Bergstrom, D.E. & Barany, F. Improving the fidelity of *Thermus thermophilus* DNA ligase. *Nucleic Acids Res.* **24**, 3071–3078 (1996).
28. Shuman, S. Vaccinia virus DNA ligase: specificity, fidelity, and inhibition. *Biochemistry (Moscow)* **34**, 16138–16147 (1995).
29. Sriskanda, V. & Shuman, S. Specificity and fidelity of strand joining by *Chlorella* virus DNA ligase. *Nucleic Acids Res.* **26**, 3536–3541 (1998).
30. Kwok, S. *et al.* Effects of primer-template mismatches on the polymerase chain reaction: human immunodeficiency virus type 1 model studies. *Nucleic Acids Res.* **18**, 999–1005 (1990).
31. Coco, W.M., Crist, M., Levinson, W.E. & Darzins, A. A novel method of gene family shuffling relieves simultaneous bottlenecks in a highly engineered pathway. In *Abstracts of the Society for Industrial Microbiology Annual Meeting*, San Diego, Abstr. P30 97. (Society for Industrial Microbiology, Fairfax, VA; 2000).
32. Moore, J.C., Jin, H.M., Kuchner, O. & Arnold, F.H. Strategies for the *in vitro* evolution of protein function: enzyme evolution by random recombination of improved sequences. *J. Mol. Biol.* **272**, 336–347 (1997).
33. Sambrook, J., Fritsch, E.F. & Maniatis, T. *Molecular Cloning*, Edn. 2. (Cold Spring Harbor Laboratory Press, Plainview, New York; 1989).
34. Liu, W.E., Tan, D. & Zhang, Z. Serum HBV DNA detected by polymerase chain reaction with dUTP/uracil–DNA glycosylase. *Hunan I. Ko Ta Hsueh Hsueh Pao* **23**, 278–280 (1998).
35. Lyamichev, V., Brow, M.A. & Dahlberg, J.E. Structure-specific endonucleolytic cleavage of nucleic acids by eubacterial DNA polymerases. *Science* **260**, 778–783 (1993).
36. Bigey, F., Grossiord, B., Chan Kuo Chion, C.K., Arnaud, A. & Galzy, P. *Brevibacterium linens* pBL33 and *Rhodococcus rhodochrous* pRC1 cryptic plasmids replicate in *Rhodococcus* sp. R312 (formerly *Brevibacterium* sp. R312). *Gene* **154**, 77–79 (1995).
37. O'Connor, K.E., Dobson, A.D. & Hartmans, S. Indigo formation by microorganisms expressing styrene monooxygenase activity. *Appl. Environ. Microbiol.* **63**, 4287–4291 (1997).

Protein family review

Cytochromes P450: a success story

Danièle Werck-Reichhart* and René Feyereisen†

Addresses: *Department of Stress Response, Institute of Plant Molecular Biology, CNRS-FRE2161, rue Goethe, 67083 Strasbourg Cedex, France. †INRA, Centre de Recherches d'Antibes, Route de Biot, 06560 Valbonne, France.

Correspondence: Danièle Werck-Reichhart. E-mail: daniele.werck@ibmp-ulp.u-strasbg.fr

Published: 8 December 2000

Genome Biology 2000, 1(6):reviews3003.1-3003.9

The electronic version of this article is the complete one and can be found online at <http://genomebiology.com/2000/1/6/reviews/3003>

© GenomeBiology.com (Print ISSN 1465-6906; Online ISSN 1465-6914)

Summary

Cytochrome P450 proteins, named for the absorption band at 450 nm of their carbon-monoxide-bound form, are one of the largest superfamilies of enzyme proteins. The P450 genes (also called *CYP*) are found in the genomes of virtually all organisms, but their number has exploded in plants. Their amino-acid sequences are extremely diverse, with levels of identity as low as 16% in some cases, but their structural fold has remained the same throughout evolution. P450s are heme-thiolate proteins; their most conserved structural features are related to heme binding and common catalytic properties, the major feature being a completely conserved cysteine serving as fifth (axial) ligand to the heme iron. Canonical P450s use electrons from NAD(P)H to catalyze activation of molecular oxygen, leading to regiospecific and stereospecific oxidative attack of a plethora of substrates. The reactions carried out by P450s, though often hydroxylation, can be extremely diverse and sometimes surprising. They contribute to vital processes such as carbon source assimilation, biosynthesis of hormones and of structural components of living organisms, and also carcinogenesis and degradation of xenobiotics. In plants, chemical defense seems to be a major reason for P450 diversification. In prokaryotes, P450s are soluble proteins. In eukaryotes, they are usually bound to the endoplasmic reticulum or inner mitochondrial membranes. The electron carrier proteins used for conveying reducing equivalents from NAD(P)H differ with subcellular localization. P450 enzymes catalyze many reactions that are important in drug metabolism or that have practical applications in industry; their economic impact is therefore considerable.

Gene organization and evolutionary history

P450 superfamily genes are subdivided and classified following recommendations of a nomenclature committee [1,2] on the basis of amino-acid identity, phylogenetic criteria and gene organization. The root symbol *CYP* is followed by a number for families (generally groups of proteins with more than 40% amino-acid sequence identity, of which there are over 200), a letter for subfamilies (greater than 55% identity) and a number for the gene; for example, *CYP4U2*. There are also designations for clades of *CYP* families (clans, which can be defined as groups of genes that clearly diverged from a single common ancestor; clans are named from the lowest

family number in the clade) [3] and for specific alleles of a gene (in humans) [4,5]. The diversity of the cytochrome P450 superfamily arose by an extensive process of gene duplications and by probable, but less well documented, cases of gene amplifications, conversions, genome duplications, gene loss and lateral transfers. 'Fossil' evidence of these processes can be found by careful sequence alignments as well as from the presence of many P450 gene clusters in most organisms. These gene clusters can contain up to 15 P450 genes, the orientation and sequence similarity of which sometimes allows a reconstruction of the events leading to the formation of the cluster. For instance in maize, four clustered *CYP71C* genes

are involved in a common biosynthetic pathway for the defense compound 2,4-dihydroxy-1,4-benzoxazin-3-one (DIBOA) [6], but in most cases there is no evidence for a functional link between members of a cluster of P450 genes.

The origin of the P450 superfamily lies in prokaryotes, before the advent of eukaryotes and before the accumulation of molecular oxygen in the atmosphere. Although *Escherichia coli* has no P450 gene, *Mycobacterium tuberculosis* has 20 [7], baker's yeast has three, and the fruit fly *Drosophila melanogaster* has 83 P450 genes [8] and seven pseudogenes. The fly situation seems the norm in 'higher' animals, with about 80 P450 genes in the nematode *Caenorhabditis elegans* and about 55 genes and 25 pseudogenes in humans. Higher plants have many more P450 genes, with about 286 in *Arabidopsis thaliana* [8]. The plant P450s are polyphyletic, with one large clade, the A-type P450s, representing plant-specific enzymes involved mostly in the biosynthesis of natural products, and several other P450s (the non-A-type) being phylogenetically related to P450s from other phyla, often with some conservation of function (fatty acid or sterol metabolism). Only one P450 gene family, *CYP51*, is conserved across phyla, from plants to fungi and animals, and a *CYP51* ortholog has also been found in the bacterium *M. tuberculosis*, possibly as a result of lateral gene transfer from its host. *CYP51* genes encode the 14 α -demethylases of sterols that streamline the α -face of sterols [9]. In mammals, *CYP51* is also involved in the synthesis of meiosis-activating sterols in oocytes and testis. The complex catalytic function of *CYP51* (sequential hydroxylations followed by carbon-carbon bond cleavage) is a highly specialized, and thus derived, trait that evolved early in the eukaryotic lineage. It was lost in insects and nematodes, which are sterol heterotrophs. Various cladograms illustrating the concept of clans or several specific aspects of P450 evolution can be found in [2,6,9-12].

The exon-intron organization of P450 genes reveals a remarkable diversity of gene structure, and few, if any, intron positions are conserved between divergent P450 families [9-11,13]. Thus, the evolutionary history of P450 genes is one of multiple intron gain and loss.

Characteristic structural features

P450s can be divided into four classes depending on how electrons from NAD(P)H are delivered to the catalytic site. Class I proteins require both an FAD-containing reductase and an iron sulfur redoxin. Class II proteins require only an FAD/FMN-containing P450 reductase for transfer of electrons. Class III enzymes are self-sufficient and require no electron donor, while P450s from class IV receive electrons directly from NAD(P)H. This classification of the interactions with redox partners is unrelated to P450 evolutionary history.

Sequence identity among P450 proteins is often extremely low and may be less than 20%, and there are only three

absolutely conserved amino acids. The determination of an increasing number of P450 crystal structures, however, shows that this unusual variability does not preclude a high conservation of their general topography and structural fold [14]. Highest structural conservation is found in the core of the protein around the heme and reflects a common mechanism of electron and proton transfer and oxygen activation. The conserved core is formed of a four-helix (D, E, I and L) bundle, helices J and K, two sets of β sheets, and a coil called the 'meander'. These regions comprise (Figures 1,2a): first, the heme-binding loop, containing the most characteristic P450 consensus sequence (Phe-X-X-Gly-X-Arg-X-Cys-X-Gly), located on the proximal face of the heme just before the L helix, with the absolutely conserved cysteine that serves as fifth ligand to the heme iron; second, the absolutely conserved Glu-X-X-Arg motif in helix K, also on the proximal side of heme and probably needed to stabilize the core structure; and finally, the central part of the I helix, containing another consensus sequence considered as P450 signature (Ala/Gly-Gly-X-Asp/Glu-Thr-Thr/Ser), which corresponds to the proton transfer groove on the distal side of the heme.

The most variable regions are associated with either amino-terminal anchoring or targeting of membrane-bound proteins, or substrate binding and recognition; the latter regions are located near the substrate-access channel and catalytic site and are often referred to as substrate-recognition sites or SRSs [15]. They are described as flexible, moving upon binding of substrate so as to favor the catalytic reaction. Other variations reflect differences in electron donors, reaction catalyzed or membrane localization (Figure 1b). Most eukaryotic P450s are associated with microsomal membranes, and very frequently have a cluster of prolines (Pro-Pro-X-Pro) that form a hinge, preceded by a cluster of basic residues (the halt-transfer signal) between the hydrophobic amino-terminal membrane anchoring segment and the globular part of the protein (Figure 1a). Additional membrane interaction seems to be mediated essentially by a region, located between the F and G helices, that shows increased hydrophobicity [16]. A signature for mitochondrial enzymes is, in addition to an amino-terminal cleavable signal peptide, the presence of two positive charges, usually arginines, at the beginning of the L helix. Such positive charges are also found in soluble bacterial P450s of class I, which receive their electrons from a ferredoxin. Strong variation from consensus in the core region, particularly an I helix lacking the characteristic threonine and surrounding residues, is characteristic of enzymes of class III catalyzing the rearrangement of hydroperoxides. These P450s do not require molecular oxygen nor electron donor for catalysis, which explains their unusual deviation from the canonical primary structure.

No class III P450 has been crystallized to date. The crystal structures of model proteins belonging to the three other classes are, however, available [17,18], including the substrate, oxygen and CO-bound, and activated reaction-intermediate

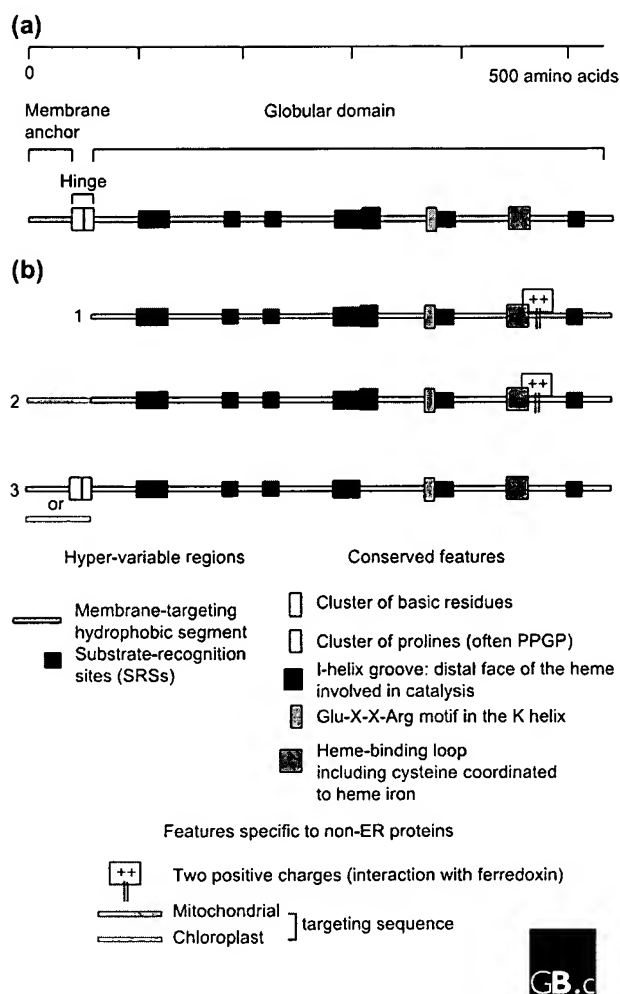


Figure 1
Primary structures of P450 proteins. **(a)** Typical features of an ER-bound P450 protein (class II enzyme). The function of the different domains and regions indicated by colors are described in the text. **(b)** Variants of this canonical structure most commonly found: 1, soluble class I; 2, mitochondrial class I; 3, membrane-bound or plastidial class III. The three-dimensional folding of these structures can be viewed at [17,18]. A good (model) picture of membrane-bound P450 can be seen at [36].

forms of some enzymes (for example class I: P450cam or CYP101 [19,20]; class II: P450BM3 or CYP102 [16,21,22]; class IV: P450nor or CYP55A1 [23]). Prototype secondary and three-dimensional structures are shown in Figure 2.

Localization and function

P450s in prokaryotes are soluble proteins. Class I P450s require both an FAD-containing NAD(P)H-reductase and an iron-sulfur redoxin as electron donors. Prokaryotic class II require only an FAD/FMN-containing NADPH-P450

reductase, which is fused to the P450 protein. P450s often confer on prokaryotes the ability to catabolize compounds used as carbon source or to detoxify xenobiotics. Other functions described for prokaryotic P450s include fatty acid metabolism and biosynthesis of antibiotics.

Eukaryotic class I enzymes are found associated with the inner membrane of mitochondria and catalyze several steps in the biosynthesis of steroid hormones and vitamin D₃ in mammals. Mitochondrial P450s are also found in insects and nematodes, but so far none has been described in plants. Animal mitochondrial P450s appear to have evolved by mis-targeting of an animal microsomal P450, and they are not phylogenetically related to the class I P450s of bacteria despite their analogous electron transport chain. Class II enzymes are the most common in eukaryotes. P450s and NADPH-P450 reductases are dissociated and independently anchored on the outer face of the endoplasmic reticulum (ER) by amino-terminal hydrophobic anchors. An additional carboxy-terminally ER-anchored electron donor, cytochrome b₅, which conveys electrons from NAD(P)H, has been found to enhance the activity of some P450 enzymes. Functions of enzymes of class II are extremely diverse. In fungi, they include synthesis of membrane sterols and mycotoxins, detoxification of phytoalexins, and metabolism of lipid carbon sources. In animals, physiological functions include many aspects of the biosynthesis and catabolism of signalling molecules, steroid hormones, retinoic acid and oxylipins [2,24,25]. Class II P450s from plants are involved in biosynthesis or catabolism of all types of hormones, in the oxygenation of fatty acids for the synthesis of cutins, and in all of the pathways of secondary metabolism - in lignification and the synthesis of flower pigments and defense chemicals (which are also aromas, flavors, antioxidants, phyto-estrogens, anti-cancer drugs and other drugs) [12,26]. Class I and class II P450s from all organisms participate in the detoxification or sometimes the activation of xenobiotics. They have been shown to contribute to carcinogenesis, and are essential determinants of drug and pesticide metabolism, tolerance, selectivity and compatibility [24,25,27,28]. P450s that actively metabolize xenobiotics often have their expression induced by exogenous chemicals [25,28-30]. Their pharmacologic and agronomic impact is thus considerable.

P450s from class III are self-sufficient and do not require molecular oxygen or an external electron source. They catalyze the rearrangement or dehydration of alkylhydroperoxides or alkylperoxides initially generated by dioxygenases [31]. These enzymes are involved in the synthesis of signalling molecules such as prostaglandins in mammals and jasmonate in plants; they seem to have diverse subcellular localizations in plants, including plastidial. A P450 that receives its electrons directly from NADH has also been described that belongs to class IV. This unique fungal P450 is soluble and reduces NO generated by denitrification to N₂O [31]. The latter two classes might be considered as

remains of the most ancestral forms of P450 involved in detoxification of harmful activated oxygen species.

There is no rule for the tissue distribution of P450 enzymes. As their functions are extremely diverse, they can be found in all types of tissues, with developmentally regulated patterns of expression, in all types of organisms. They were first described in mammalian liver where they are especially abundant and play an essential role in drug metabolism [32,33].

A list of selected mutant phenotypes that illustrate the various functions of P450 proteins is given in Table 1.

Enzyme mechanism

P450 enzymes have been compared to a blowtorch. They catalyze regiospecific and stereospecific oxidative attack of non-activated hydrocarbons at physiological temperatures. Such a reaction, uncatalyzed, would require extremely high temperature and would be nonspecific. The details of the mechanism by which P450s carry out all types of reactions, especially the most complex ones found in plants, are not yet understood. The best documented aspect is the oxygen activation that is common to most P450s, including soluble enzymes for which crystal structures of different forms have been obtained. The active center for catalysis is the iron-protoporphyrin IX (heme) with the thiolate of the conserved cysteine residue as fifth ligand. Resting P450 is in the ferric form and partially six-coordinated with a molecule of solvent (Figure 3).

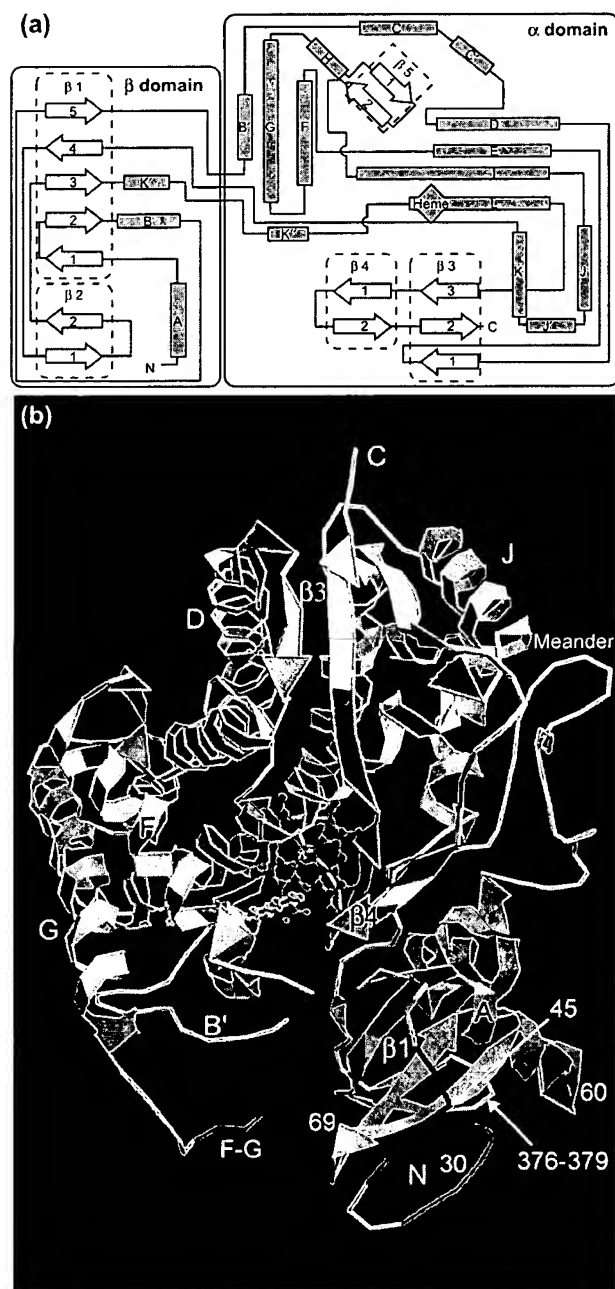


Figure 2

Secondary and tertiary structures of P450 proteins.

(a) Topology diagram showing the secondary structure and arrangement of the secondary structural elements of a typical P450 protein (CYP102) [14]. Blue boxes, α helices; groups of cream arrows outlined with dotted lines, β sheets; lines, coils and loops. The sizes of the elements are not in proportion to their length in the primary sequence. There are usually around four β sheets and 13 α helices defining one domain that is predominantly β sheets and one that is predominantly α helices. The first domain is often associated with substrate recognition and the access channel, the second with the catalytic center. Adapted from [14]. (b) A ribbon representation of the distal face of the folded CYP2C5 protein showing its putative association with the ER membrane (purple) [16]. Helices and sheets are labeled as in (a). Heme is in orange, the substrate in yellow. The α domain is on top left, the β domain more closely associated with the membrane at bottom right. Epitopes not accessible for antibody binding when the protein is associated with the ER are shown in red (numbers give their position in the primary sequence). The transmembrane amino-terminal segment, removed for crystallization, and an additional 11 residues that are disordered in the crystal structure, are not shown. Note the I helix above the heme, close to the substrate-binding site. The heme-binding loop is visible behind the heme protoporphyrin. The conserved Gln-X-X-Arg structure in the K helix is also at the back and so is not readily visible. The proximal (back) face of the protein is involved in redox partner recognition and electron transfer to the active site; protons flow into the active site from the distal face (front). The substrate access channel is usually assumed to be located in close contact of the membrane between the F-G loop, the A helix and β strands 1-1 and 1-2. More pictures showing other aspects of the structure, including reductase and substrate-binding, can be viewed at [17,18]. Another picture (a model) of membrane-bound P450 including the transmembrane domain can be seen at [36]. Reproduced with permission from [37].

Table 1

Selected examples of P450 mutants characterized in various organisms

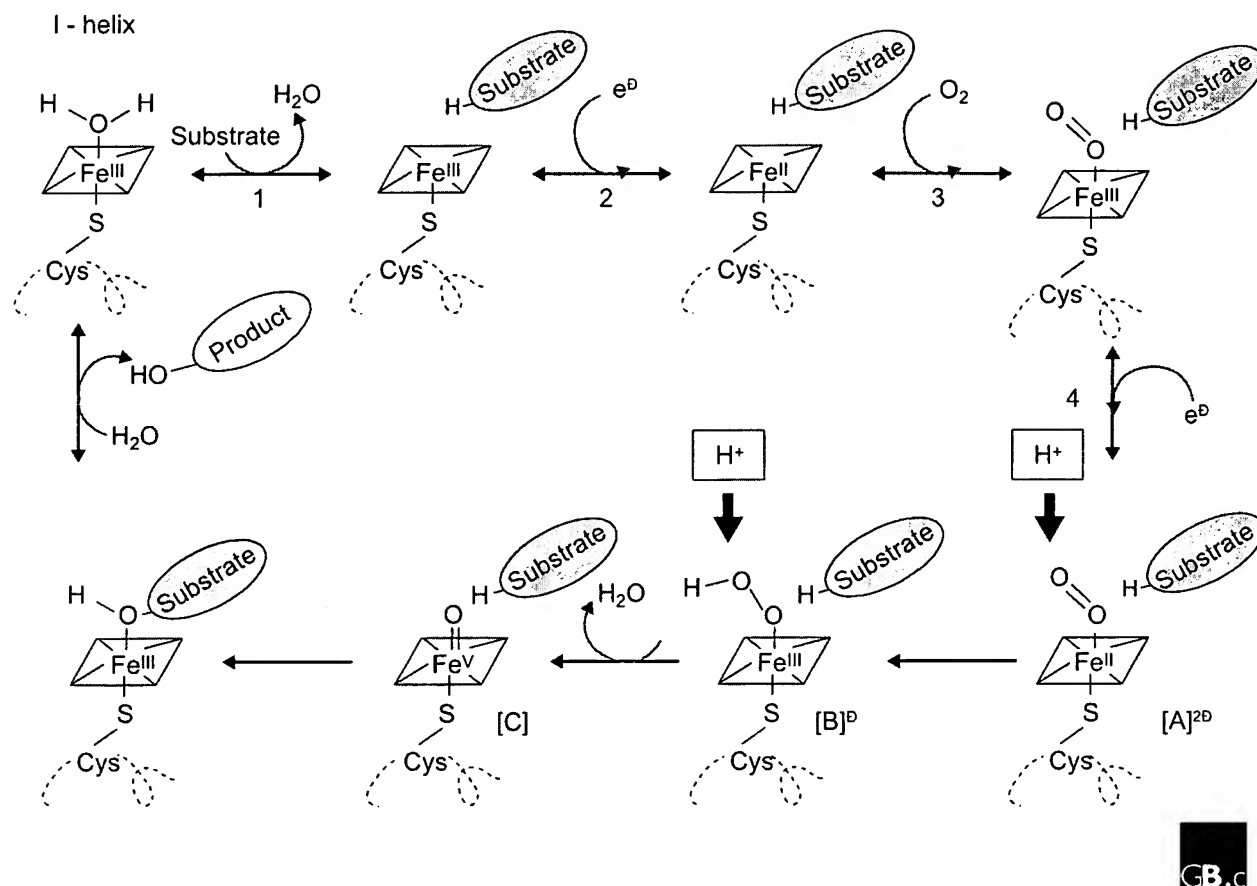
P450 mutation (mutant name)	Organism	Phenotype	Function altered	Reference
CYP1B1 defect	Human	Congenital glaucoma	Unknown	[38]
CYP17 (more than 20 alleles) (some allelic variants)	Human	Sex steroid production affected in both sexes	Steroid 17 α -hydroxylase and 17, 20-lyase	
CYP19 defect (overactive)	Human	Failure of normal female development Male feminization	Aromatase (aromatizes ring A of steroids, thus producing estrogens)	[39] [40]
CYP51 (resistant variants with point mutations)	<i>Ucinula necator</i> (powdery mildew)	Azole fungicide resistance	Eburicol 14 α -demethylase	[41]
CYP84A1 defect (EMS mutant <i>fah1</i>)	<i>A. thaliana</i>	Does not accumulate sinapoyl malate; altered lignin composition	Coniferyl aldehyde 5-hydroxylase	[42]
CYP90A1 defect (via T-DNA tagging, <i>cpd</i>)	<i>A. thaliana</i>	De-etiolated in dark and dwarfism; male sterility in the light	Brassinolide 23-hydroxylase (synthesis of steroid hormones)	[43]
CYP71C2 defect (transposon-tagged mutant, <i>Bx3::Mu</i>)	Maize	Defect in the production of DIMBOA*, more susceptible to pathogens	Indolin-2-one 3-hydroxylase	[6]
CYP72B1 overactive (activation tagging, <i>bas1-D</i>)	<i>A. thaliana</i>	Suppression of long hypocotyl phenotype of photoreceptor phyB-4 mutant	Brassinolide 26-hydroxylase (catabolism of brassinosteroids)	[44]
CYP75A1 (breeding mutants; 2 alleles, <i>Hf1</i> and <i>Hf2</i>)	<i>Petunia</i>	Altered flower color (blue to pink)	Flavonoid 3',5'-hydroxylase	[45]
CYP302A1 defect (EMS mutants)	<i>Drosophila melanogaster</i>	Embryonic morphogenesis and cuticle deposition impaired	Probable enzyme in the pathway of ecdysteroid (insect molting hormone) biosynthesis	[46]
CYP504 (disruption)	<i>Aspergillus nidulans</i>	Penicillin overproduction	Phenylacetate 2-hydroxylase (a reaction competing with antibiotic biosynthesis)	[47]

This is not an exhaustive list, but is only meant to provide a glimpse of the functional diversity of P450 enzymes. *2,4-dihydroxy-7-methoxy-1,4-benzoxazin-3-one (DIMBOA) is one of the major defense compounds against microbial pathogens and insects accumulated in the gramineae.

The well characterized portion of the catalytic sequence involves four steps, which are indicated in Figure 3. The first step is substrate binding, with displacement of the sixth ligand solvent inducing a shift in the maximum of absorbance, spin state and redox potential of the heme protein system; the second is one-electron reduction of the complex to a ferrous state, driven by the increase in redox potential that results from the previous step; the third is binding of molecular oxygen to give a superoxide complex; and the fourth is a second reduction step leading to an 'activated oxygen species'. The exact nature of the very short-lived activated oxygen species that carries on substrate attack long remained uncertain, but the most recent data, from crystallography and mechanistic probes [20,34], strongly suggest that it is actually a mixture of two electrophilic oxidants ([B]⁻ and [C] in Figure 3). Both iron-peroxo [B]⁻ and iron-oxo [C] complexes are formed by protonation of the two-electrons-reduced dioxygen, a process that is allowed when a water channel forms in the groove of the I-helix upon binding of O₂.

The oxo (oxyferryl) species, resulting from the cleavage of the O-O bond - one atom of oxygen leaves with the two electrons and two protons as water - is apparently the most abundant. The iron-hydroperoxo species inserts the elements of OH⁺, producing protonated alcohols that can give cationic rearrangement products. The iron-oxo species inserts an oxygen atom. The result of P450 catalysis is not always insertion of oxygen, but can be a dealkylation, dehydration, dehydrogenation, isomerization, dimerization, carbon-carbon bond cleavage, and even a reduction [31]. The substrate specificity and type of reaction catalyzed are governed by the less conserved regions of the protein and are therefore not well understood.

Carbon monoxide can bind ferrous P450 instead of dioxygen, inducing a shift of the maximum of absorbance of the heme (called the Soret peak) to 450 nm [32,33] (this property is a characteristic of P450 enzymes). CO is bound with high affinity and prevents binding and activation of O₂. The

**Figure 3**

Catalytic mechanism of P450 enzymes. P450s are usually mono-oxygenases, catalyzing the insertion of one of the atoms of molecular oxygen into a substrate, the second atom of oxygen being reduced to water. The most frequently catalyzed reaction is hydroxylation (O insertion) using the very reactive and electrophilic iron-oxo intermediate (species [C], bottom row). The hydroperoxo form of the enzyme (species [B]) is also an electrophilic oxidant catalyzing OH^+ insertion. Nucleophilic attack can be catalyzed by species $[\text{A}]^{2-}$ and [B]; reduction, isomerization or dehydration are catalyzed by the oxygen-free forms of the enzyme. This, together with the variety of the apoproteins and intrinsic reactivity of all their substrates explains the extraordinary diversity of reactions catalyzed by P450 enzymes.

result is an inhibition of P450 activity. CO binding and inhibition can be reversed by light, with maximal efficiency at 450 nm. Other ligands, substrates and inhibitors, induce absorbance shifts of the Soret in P450 enzymes. Differential spectrophotometry is thus widely used to monitor binding of such ligands [35]. Substrates that displace the six-coordinated solvent in the resting P450 usually induce a shift to the blue (420 to 390 nm) which reflects a low- to high-spin transition of the iron. Inhibitors with an sp_2 hybridized nitrogen (nitrogens in heterocycles such as azoles, pyridines, or pyrimidines) replace the sixth ligand for coordination with iron and induce a shift to the red (400 to 430 nm).

Frontiers

Issues most studied

Medical, pharmacological and toxicological studies of P450 enzymes and genes for the prediction of drug metabolism and the prevention of adverse drug reactions remain a key field of investigation. For instance, there are many allelic variants of the human *CYP2D6* gene, which encodes a liver enzyme that metabolizes a quarter of all known drugs. The *CYP2D6* genotype will determine a person's response to important drugs, such as antipsychotics and antidepressants. Another very active field is the tailoring of P450 enzymes for specific functions, via site-directed mutagenesis or *in vitro* directed evolution. The development of new approaches to improve solubility and implement crystallization of membrane-bound enzymes probably opens a new era for the understanding of

P450 mechanisms and substrate specificity, as well as engineering of such catalytic properties.

Major unresolved questions

A major unresolved issue in the field is the physiological function of many of the newly discovered P450 enzymes. Whereas this question can be practically addressed in microorganisms or other organisms amenable to homologous recombination, this is not the case in most eukaryotes such as humans, where the endogenous substrate(s) of many enzymes that have been extensively studied for xenobiotic metabolism are still unknown. Also, the molecular basis and impact of receptor-mediated transcriptional activation of many P450 genes remains a challenging area of research. An interesting point to clarify is the subcellular localization of some P450 enzymes, some of which might have more than one localization. Many P450-catalyzed reactions in plants generate compounds that might be toxic if released in the cytoplasm. There is increasing evidence of the channeling of such compounds inside multi-enzyme complexes. How do P450s interact with such complexes, and do they serve to anchor them on membranes? From a mechanistic point of view, simple hydroxylation reactions are now rather well understood. More complex reactions, for example multi-step reactions or those involving no overt oxygen insertion, are still a very open field of investigation.

References

- Nelson DR, Koymans L, Kamataki T, Stegeman JJ, Feyereisen R, Waxman DJ, Waterman MR, Gotoh O, Coon MJ, Estabrook RW, et al.: **P450 superfamily: update on new sequences, gene mapping, accession numbers and nomenclature.** *Pharmacogenetics* 1996, **6**:1-42.
This paper defines the rules for P450 gene nomenclature, comments on some general characteristics of the P450 gene superfamily, and gives a list (with references) of P450 genes identified in various organisms.
- David Nelson's homepage
[http://drnelson.utmem.edu/CytochromeP450.html]
David Nelson keeps an update of P450 sequences characterized in all organisms and is also the 'P450 nomenclature committee', the person to contact to obtain a name for a new P450 sequence. Nelson also provides a simple introductory lecture on mammalian P450 enzymes and on all their physiological and other functions.
- Nelson DR: **Cytochrome P450 and the individuality of species.** *Arch Biochem Biophys* 1999, **369**:1-10.
This paper defines the clans in P450 classification and gives some examples. In addition to evolutionary considerations, it comments on new P450 genes and functions recently discovered and on P450 polymorphism and its impact on drug metabolism.
- Ingelman-Sundberg M, Daly AK, Oscarson M, Nebert D: **Human cytochrome P450 (CYP) gene: recommendations for the nomenclature of alleles.** *Pharmacogenetics* 2000, **10**:91-93.
This paper and the related website [6] give rules and examples for the nomenclature of P450 alleles.
- Home Page of the Human Cytochrome P450 (CYP) Allele Nomenclature Committee [http://www.imm.ki.se/CYPalleles/]
An update of the knowledge on allelic variants of the human genes; also provides instructions on the submission of new variants.
- Frey M, Chomet P, Glawischig E, Stettner C, Grün S, Winklmeier A, Eisenreich W, Bacher A, Meeley R B, Briggs SB, et al.: **Analysis of a chemical plant defense mechanism in grasses.** *Science* 1997, **277**:696-699.
The first analysis of a P450 gene cluster in plants (maize). Provides evidence that four evolutionary related P450 genes, belonging to same sub-family and clustered on the same chromosome, catalyze four successive steps in a single pathway.
- Directory of P450-containing systems**
[http://www.icgeb.trieste.it/~p450srv/]
Lists P450 and related genes. More information on P450 structure, ligands, domain structure, electron donors and useful links on human alleles, drug metabolism, commercially available forms; also contains references.
- The P450 site at the University of Arizona**
[http://ag.arizona.edu/p450/]
A site with a list, annotation and a physical map of *Drosophila* and *A. thaliana* P450s.
- Rozman D, Stromstedt M, Tsui LC, Scherer SW, Waterman MR: **Structure and mapping of the human lanosterol 14 α -demethylase gene (CYP51) encoding the cytochrome P450 involved in cholesterol biosynthesis; comparison of exon/intron organization with other mammalian and fungal CYP genes.** *Genomics* 1996, **38**:371-381.
Provides a detailed analysis of a human P450 gene structure and comparative analysis of P450 gene structures in mammals and fungi.
- Paquette SM, Bak S, Feyereisen R: **Intron-exon organization and phylogeny in a large superfamily, the paralogous cytochrome P450 genes of *Arabidopsis thaliana*.** *DNA Cell Biol* 2000, **19**:307-317.
Provides a detailed analysis of the P450 gene family in *A. thaliana*: gene mapping, phylogeny and intron-exon organization.
- Tijet N, Helvig C, Feyereisen R: **The cytochrome P450 gene superfamily in *Drosophila melanogaster*: annotation, intron-exon organization and phylogeny.** *Gene* 2000, in press.
A complete report on the microsomal and mitochondrial P450s of the fruit fly, their gene structures and their distribution in the genome.
- Chapple C: **Molecular genetics analysis of plant cytochrome P450-dependent monooxygenases.** *Ann Rev Plant Physiol Mol Biol* 1998, **49**:311-343.
Provides some basic information on P450 characteristics and nomenclature; gives a list of plant P450 genes and mutants already isolated and their functions.
- Gotoh O: **Divergent structures of *Caenorhabditis elegans* cytochrome P450 genes suggest the frequent loss and gain of introns during the evolution of nematodes.** *Mol Biol Evol* 1998, **15**:1447-1459.
An extensive study of gene structure in the nematode, with a thorough discussion of the process of intron gain and loss in the P450 superfamily.
- Graham SE, Peterson JA: **How similar are P450s and what can their differences teach us.** *Arch Biophys Biochem* 1999, **369**:24-29.
A recent overview of the available data on P450 three-dimensional structure, comparison of the different crystallized structures in view of substrate specificity and redox partners of the different forms.
- Gotoh O: **Substrate recognition sites in cytochrome P450 family 2 (CYP2) protein inferred from comparative analyses of amino acid and coding nucleotide sequences.** *J Biol Chem* 1992, **267**:83-90.
The reference paper defining the hyper-variable substrate recognition sites (SRSS).
- Williams PA, Cosme J, Sridhar V, Johnson E, McRee DE: **Mammalian microsomal cytochrome P450 monooxygenase: structural adaptations for membrane binding and functional diversity.** *Mol Cell* 2000, **5**:121-131.
First structural report on a microsomal enzyme: describes similarities and difference with the soluble forms.
- Julian A ('Bill') Peterson's home page
[http://p450terp.swmed.edu/Bills_folder/billhome.htm]
An easy access to didactic pictures illustrating P450 interaction with the P450-reductase and active-site structure.
- The Scripps Institute P450 protein site**
[http://metallo.scripps.edu/PROMISE/P450.html]
Information on prosthetic group, different P450 types, reaction catalyzed, P450 enzyme, motif and alignment databases, three-dimensional (3D) structure databases and structural references.
- Poulos TL, Finzel B C, Gunsalus IC, Wagner GC, Kraut J: **The 2.6-Å crystal structure of *Pseudomonas putida* cytochrome P-450.** *J Biol Chem* 1985, **260**:16122-16130.
The first high-resolution structure of a bacterial soluble (class I) P450.
- Schlichting I, Berendzen J, Chu K, Stock AM, Maves SA, Benson DE, Sweet RM, Ringe D, Petsko GA, Sligar SG: **The catalytic pathway of cytochrome P450cam at atomic resolution.** *Science* 2000, **287**:1615-1622.
The most recent update on the 3D structure of class I bacterial enzymes: includes the structure of one-electron-reduced forms and of the activated oxygen complex. Two forms of activated oxygen are detected in the crystal, confirming the biochemical data of [35].

21. Ravichandran KG, Boddupalli SS, Hasemann CA, Peterson JA, Deisendorfer J: **Crystal structure of hemoprotein domain of P450BM-3, a prototype for microsomal P450's.** *Science* 1993, **261**:731-736.
The first description of the 3D structure of a class II enzyme. Until the coordinates of the mammalian CYP2C5 become available, probably in the next year, this serves as a reference for the eukaryotic membrane-bound enzymes.
22. Li H, Poulos TL: **The structure of the cytochrome P450BM-3 haem domain complexed with the fatty acid substrate, palmitoleic acid.** *Nat Struct Biol* 1997, **4**:140-146.
A very interesting description of the class II enzyme crystallized with its substrate. A model for fatty-acid-metabolizing P450s in all kingdoms, providing the first detailed picture of substrate-induced conformational changes in a P450.
23. Park SY, Shimizu H, Adachi S, Nakagawa A, Tanaka I, Nakahara K, Shoun H, Obayashi E, Nakamura H, Iizuka T, Shiro Y: **Crystal structure of nitric oxide reductase from denitrifying fungus *Fusarium oxysporum*.** *Nat Struct Biol* 1997, **10**:827-832.
First description of the 3D structure of a class IV enzyme. Provides evidence of significant differences in proton delivery and access of NADH to the active site.
24. Hasler JA, Estabrook R, Murray M, Pikuleva I, Waterman M, Capdevila J, Holla V, Helvig C, Falck JR, Farrell G, et al.: **Human cytochromes P450.** *Mol Aspects Med* 1999, **20**:1-137.
A very complete overview of P450 roles in human normal physiology, pathology and drug metabolism.
25. Feyereisen R: **Insect cytochrome P450 enzymes.** *Annu Rev Entomol* 1999, **44**:507-533.
Provides a review of the physiological functions of insect P450 as well as the role and regulation of P450 in insecticide metabolism, insecticide resistance, and the adaptation to plant chemicals.
26. Kahn R, Durst F: **Function and evolution of plant cytochrome P450.** *Recent Adv Phytochem* 2000, **34**:151-189.
The most recent review on the role of P450 enzymes in the biosynthesis of plant natural compounds. Also comments on plant P450 evolution and techniques useful for plant P450 gene isolation.
27. Gonzalez FJ, Kimura S: **Role of gene knockout mice in understanding the mechanisms of chemical toxicity and carcinogenesis.** *Cancer Lett* 1999, **143**:199-204.
Provides a description of the gene disruption technology in the mouse and its application for the study of three P450 genes involved in xenobiotic metabolism.
28. Werck-Reichhart D, Hehn H, Didierjean L: **Cytochromes P450 for engineering herbicide tolerance.** *Trends Plant Sci* 2000, **5**:116-123.
Reviews available data in the metabolism of exogenous compounds, in particular herbicides, in higher plants and the impact of altered metabolism on weed resistance.
29. Waxman DJ: **P450 gene induction by structurally diverse xenochemicals: central role of nuclear receptors CAR, PXR, and PPAR.** *Arch Biochem Biophys* 1999, **369**:11-23.
Summarizes recent progress in nuclear receptor driven regulation of mammalian P450s by xenochemicals. The expression of different P450 families is driven by specific nuclear receptors of the family NRI activated by exogenous and endogenous ligands.
30. Honkakoski P, Negishi M: **Regulation of cytochrome P450 genes by nuclear receptors.** *Biochem J* 2000, **347**:321-337.
Gives an overview of the nuclear receptors involved in P450 gene regulation, of their respective role in endobiotic and xenobiotic metabolism, with emphasis on the potential impact of exogenous compounds on cellular homeostasis.
31. Mansuy D: **The great diversity of reactions catalyzed by cytochrome P450.** *Comp Biochem Physiol Part C* 1998, **121**:5-14.
A good simplified overview on the diversity and mechanism of reaction catalyzed by P450 enzymes.
32. Klingenberg M: **Pigments of rat liver microsomes.** *Arch Biochem Biophys* 1958, **75**:376-386.
First description of a pigment absorbing at 450 nm when reduced in mammalian liver microsomes.
33. Omura T, Sato R: **The carbon monoxide-binding pigment of liver microsomes. I. Evidence for its hemoprotein nature.** *J Biol Chem* 1964, **239**:2370-2378.
Demonstration of the hemoprotein nature of the pigment absorbing at 450 nm; gives the extinction coefficient used for all P450 quantifications.
34. Newcomb M, Shen R, Choi S-Y, Toy PH, Hollenberg PF, Vaz ADN, Coon MJ: **Cytochrome P450-catalyzed hydroxylation of mechanistic probes that distinguish between radical and cations, evidence for cationic but not radical intermediates.** *J Am Chem Soc* 2000, **122**:2677-2686.
The most recent update on P450 catalytic mechanism. Provides evidence of the existence of two activated oxygen forms (iron-oxo and hydroperoxo-iron) for the same enzymes, both forms producing different products with mechanistic probes. Also gives evidence that the reaction occurs in both cases by direct insertion.
35. Jefcoate C R: **Measurement of substrate and inhibitor binding to microsomal cytochrome P450 by optical difference spectroscopy.** *Methods Enzymol* 1978, **52**:258-279.
A reference paper that provides the basis for ligand-binding detection by spectrophotometry.
36. Fred K. Friedman's Home Page
[<http://rex.nci.nih.gov/RESEARCH/basic/lm/fkf.htm>]
The place to see a model of P450 insertion in a membrane.
37. Williams PA, Cosme J, Sridhar V, Johnson EF, McRee DE: **Microsomal cytochrome P450 2C5: comparison to microbial P450s and unique features.** *J Inorg Biochem* 2000, **81**:183-190.
More pictures to illustrate the differences between microbial and membrane-bound proteins.
38. Stoilov I, Akarsu AN, Sarfarazi M: **Identification of three different truncating mutations in cytochrome P4501B1 (CYP1B1) as the principal cause of primary congenital glaucoma (Buphthalmos) in families linked to the GLC3A locus on chromosome 2p21.** *Hum Mol Genet* 1997, **4**:641-647.
Three null alleles described in five well characterized families point to the lack of CYP1B1 as causing developmental defects in the anterior anterior uveal tract, which is involved in secretion of the aqueous humor. A point mutation in CYP1B1 has since been identified at very high frequency (10%) in an ethnic isolate of Slovak Gypsies, a population with increased incidence of primary congenital glaucoma. The substrate of CYP1B1 is unknown.
39. Geller DH, Auchus RJ, Mendonça BB, Miller W: **The genetic and functional basis of isolated 17,20-lyase deficiency.** *Nat Genet* 1997, **17**:201-205.
The mammalian P450 CYP17 is an unusual P450 catalyzing two successive reactions in the biosynthesis of steroids. Its 17 α -hydroxylase activity is sufficient for the biosynthesis of glucocorticoids. Successive 17 α -hydroxylase and 17,20-lyase activities catalyzed by CYP17 are needed for the biosynthesis of steroid hormones. Here human mutants forms are described which retain normal 17 α -hydroxylase activity but are severely defective in 17,20-lyase activity. It is shown that the defect is due to a diminished ability of the P450 to interact with its redox partners.
40. Stratakis CA, Vottero A, Brodie A, Kirschner LS, DeAtkine D, Lu Q, Yue W, Mitsiades CS, Flor AW, Chrousos GP: **The aromatase excess syndrome is associated with feminization of both sexes and autosomal dominant transmission of aberrant P450 aromatase gene transcription.** *J Clin Endocrinol Metab* 1998, **83**:1348-1357.
A case of familial gynecomastia is described in which a new 5' splicing variant leads to the abnormal overexpression of an aromatase transcript with a new first exon. The excess aromatase syndrome is described in both sexes.
41. Delye C, Laigret F, Corio-Costet MF: **A mutation in the 14 α -demethylase gene of *Uncinula necator* that correlates with resistance to a sterol biosynthesis inhibitor.** *Applied Env Microbiol* 1997, **63**:2966-2970.
Resistance of the grape powdery mildew to 14 α -demethylase inhibitors such as triadimenol was correlated in multiple isolates with a single Phe137Tyr point mutation in the CYP51 gene. The same mutation can be found in other resistant fungi.
42. Chapple CCS, Vogt T, Ellis BE, Somerville CR: **An Arabidopsis mutant defective in the general phenylpropanoid pathway.** *Plant Cell* 1992, **4**:1413-1424.
Describes a recessive mutant deficient in the synthesis of sinapoyl-malate, selected on the basis of a change in leaf epidermis fluorescence (blue-green to red) under UV-light. On the basis of feeding and precursor supplementation experiments it is shown that this mutant is defective for the 5-hydroxylation step in the general phenylpropanoid pathway, a reaction previously shown to be catalyzed by a P450 enzyme. After isolation of the mutant, it took several years to identify the real substrate of the reaction, which was different from expected.
43. Szekeres M, Nemeth K, Koncs-Kalman Z, Mathur J, Kauschmann A, Altmann T, Redei GP, Nagy F, Schell J, Koncs C: **Brassinosteroids rescue the deficiency of CYP90, a cytochrome P450 control-**

ling cell elongation and de-etiolation in *Arabidopsis*. *Cell* 1996, **85**:171-182.

Describes a recessive mutant selected on the basis of hypocotyl and root elongation during skotomorphogenesis, displaying de-etiolation in the dark and dwarfism, male sterility and activation of stress-regulated genes in the light. The defect can be rescued by C23-hydroxylated brassinolide precursors, which demonstrates the involvement of the tagged gene in the biosynthesis of brassinosteroid hormones which are essential for plant development. Other P450-catalyzed steps were subsequently characterized in the same pathway using similar approaches.

44. Neff MM, Nguyen SM, Malancharuvil EJ, Fujioka S, Noguchi T, Seto H, Tsubuki M, Honda T, Takatsuto S, Chory J: **BASI: a gene regulating brassinosteroid level and light responsiveness in *Arabidopsis*.** *Proc Natl Acad Sci USA* 1999, **96**:15316-15323.

This paper reports the first functional characterization of a P450 gene by activation tagging. A dominant mutation suppresses the missense mutation in the photoreceptor phytochrome B. The mutant has no detectable brassinolide, the most active brassinosteroid hormone and accumulate a 26-hydroxylated inactive metabolite. Crosses suggest that the activated gene is a control point between photoreceptor signal transduction pathways and hormone signaling.

45. Holton TA, Brugliera F, Lester DR, Tanaka Y, Hyland CD, Menting JGT, Lu C-Y, Farcy E, Stevenson TW, Cornish EC: **Cloning and expression of cytochrome P450 genes controlling flower colour.** *Nature* 1993, **366**:276-279.

Describes the PCR-based isolation of two P450 genes complementing flower-color mutations of petunia. Provides the definitive proof that P450-dependent hydroxylation of the ring B of flavonoids is a major determinant of pink-to-blue shift of flower color.


46. Chavez VM, Marques G, Delbecque JP, Kobayashi K, Hollingsworth M, Burr J, Natzle JE, O'Connor MB: **The *Drosophila* disembodied gene controls late embryonic morphogenesis and codes for a cytochrome P450 enzyme that regulates embryonic ecdysone levels.** *Development* 2000, **127**:4115-4126.

The *dib* gene is shown to encode CYP302A1, a mitochondrial P450. Mutants at this locus have very low titers of ecdysteroids (molting hormones) and are defective in edysteroid-regulated processes such as embryonic cuticle synthesis or induction of ecdysteroid-responsive genes.

47. Mingot JM, Penalva MA, Fernandez-Canon JM: **Disruption of *phacA*, an *Aspergillus nidulans* gene encoding a novel cytochrome P450 monooxygenase catalyzing phenylacetate 2-hydroxylation, results in penicillin overproduction.** *J Biol Chem* 1999, **274**:14545-14550.

CYP504 is induced by and metabolizes phenylacetate in this aerobic fungus by a rare *ortho*-hydroxylation. This catabolism competes with the use of phenylacetate in the penicillin biosynthetic pathway, and disruption of the CYP504 gene leads to penicillin overproduction.

Tom Murphy/CHI/MWE
01/09/2006 02:08 PM

To Jacqueline D Reid-Johnson/WDC/MWE@MWE
cc
bcc
Subject Re: Shockwave applicator for Sanuwave-74636-012 

Jackie,

SanuWave is owned by Prides Capital and Chris Puscasiu is the principal of Prides that handles this investment. He was the acting CEO until a couple of weeks ago when Chris Cashman became the CEO. I'm not sure who is the appropriate person to receive the reporting letter because I'm not really sure what it is. If this is enough information for you to decide or if it possible to send it to all three (my secretary, Ardis Lozenski, has the addresses and emails) then that's fine. If you need to pick one person and still aren't sure who it should be give me a call and we can try to figure it out. Thanks a lot.

Tom

Thomas J. Murphy
McDermott Will & Emery LLP
227 West Monroe Street
Chicago, Illinois 60606
Phone: 312.984.2069
Fax: 312.984.7700
Jacqueline D Reid-Johnson/WDC/MWE



Jacqueline D
Reid-Johnson/WDC/MWE
01/09/2006 12:24 PM

To Tom Murphy/CHI/MWE@MWE
cc
Subject Shockwave applicator for Sanuwave-74636-012

Mr. Murphy,

As you are aware, our office filed a provisional application on December 30, 2005 for the above-referenced matter. We would now like to know who the reporting letter should be sent to, please advise?

We have Manfred Menzi listed as the Inventor and also Chris Puscasiu (not sure who Chris is).

Thanks
Jackie Reid-Johnson
Notary Public
Assistant to Cameron Weiffenbach, Esq.,
Thomas Haag, Ph.D., Atsushi Teraguchi and
Demetria Buncum
McDermott Will & Emery LLP
Intellectual Property Dept.
Washington, DC

jdjohnson@mwe.com
(202) 756-8668 (direct dial)
(202) 756-8087 (fax)

...Many are those who wish and want,
few are those who act and acquire...

IRS Circular 230 Disclosure: To comply with requirements imposed by the IRS, we inform you that any U.S. federal tax advice contained herein (including any attachments), unless specifically stated otherwise, is not intended or written to be used, and cannot be used, for the purposes of (i) avoiding penalties under the Internal Revenue Code or (ii) promoting, marketing or recommending to another party any transaction or matter herein.

This message is a PRIVATE communication. This message and all attachments are a private communication sent by a law firm and may be confidential or protected by privilege. If you are not the intended recipient, you are hereby notified that any disclosure, copying, distribution or use of the information contained in or attached to this message is strictly prohibited. Please notify the sender of the delivery error by replying to this message, and then delete it from your system. Thank you.

Please visit <http://www.mwe.com/> for more information about our Firm.

IRS Circular 230 Disclosure: To comply with requirements imposed by the IRS, we inform you that any U.S. federal tax advice contained herein (including any attachments), unless specifically stated otherwise, is not intended or written to be used, and cannot be used, for the purposes of (i) avoiding penalties under the Internal Revenue Code or (ii) promoting, marketing or recommending to another party any transaction or matter herein.

This message is a PRIVATE communication. This message and all attachments are a private communication sent by a law firm and may be confidential or protected by privilege. If you are not the intended recipient, you are hereby notified that any disclosure, copying, distribution or use of the information contained in or attached to this message is strictly prohibited. Please notify the sender of the delivery error by replying to this message, and then delete it from your system. Thank you.

Please visit <http://www.mwe.com/> for more information about our Firm.

p: WINWORD\memo\JUMP MEMO. DOC

(Sent to you on e mail)
letterhead on envelope.

Date: November 13, 1995

To: Adrian Hunter
Bryan Loft

CIBA
Vision

Patent Department
11460 Johns Creek Parkway
Duluth, Georgia 30155
Telephone: (770) 418-3054
Fax: (770) 418-3068

Provisional Inventors:

Paul Nicolson
Rich Baron
Qin Liu
Dieter Lohmann
Judy Riffle
Klaus Schindhelm
Lenny Terry
Jürgen Vogt
Lynn Winterton
Angelika Domschke
Jens Höpken

From: Jörg Dietz
Scott Meece

Enclosed is a copy of the revised "JUMP" patent application. Please review the disclosure for technical accuracy. Again, please pay particular attention to the specified ranges for properties and compositions.

The examples of materials are outlined below in terms of SEE3 Project names:

Material A	=	NC Alsacon
Material B	=	Betacon
Material C	=	Glycon II
Material D	=	Podium

Please return your comments with the application draft to Scott Meece at the above address. Comments must be received by Wednesday, Nov. 22 to ensure incorporation into the patent application.

No additional drafts will be sent to the provisional inventors before filing.

Please see the list of attached questions and submit any responses or comments in writing to S. Meece by November 22.

Thank you for your prompt cooperation.

Enclosure
Attachment

CV36 005901

CSFJ036697

**This Page is Inserted by IFW Indexing and Scanning
Operations and is not part of the Official Record**

BEST AVAILABLE IMAGES

Defective images within this document are accurate representations of the original documents submitted by the applicant.

Defects in the images include but are not limited to the items checked:

- ☐ **BLACK BORDERS**
- ☐ **IMAGE CUT OFF AT TOP, BOTTOM OR SIDES**
- ☐ **FADED TEXT OR DRAWING**
- ☐ **BLURRED OR ILLEGIBLE TEXT OR DRAWING**
- ☐ **SKEWED/SLANTED IMAGES**
- ☐ **COLOR OR BLACK AND WHITE PHOTOGRAPHS**
- ☐ **GRAY SCALE DOCUMENTS**
- ☐ **LINES OR MARKS ON ORIGINAL DOCUMENT**
- ☐ **REFERENCE(S) OR EXHIBIT(S) SUBMITTED ARE POOR QUALITY**
- ☐ **OTHER:** _____

IMAGES ARE BEST AVAILABLE COPY.

As rescanning these documents will not correct the image problems checked, please do not report these problems to the IFW Image Problem Mailbox.